Inorg. Chem. **2004**, *43*, 537–554

Supramolecular Structural Variations with Changes in Anion and Solvent in Silver(I) Complexes of a Semirigid, Bitopic Tris(pyrazolyl)methane Ligand

Daniel L. Reger,* Radu F. Semeniuc, Vitaly Rassolov, and Mark D. Smith

Department of Chemistry and Biochemistry, University of South Carolina, Columbia, South Carolina 29208

Received October 21, 2003

The bitopic ligand *p*-$C_6H_4[CH_2OCH_2C(pz)_3]_2$ (pz = pyrazolyl ring) that contains two tris(pyrazolyl)methane units connected by a semirigid organic spacer reacts with silver(I) salts to yield $\{p\text{-}C_6H_4[CH_2OCH_2C(pz)_3]_2(AgX)_2\}_\infty$, where X = $CF_3SO_3^-$ (**1**), SbF_6^- (**2**), PF_6^- (**3**), BF_4^- (**4**), and NO_3^- (**5**). Crystallization of the first three compounds from acetone yields $\{p\text{-}C_6H_4[CH_2OCH_2C(pz)_3]_2(AgCF_3SO_3)_2\}_\infty$ (**1a**), $\{p\text{-}C_6H_4[CH_2OCH_2C(pz)_3]_2(AgSbF_6)_2[(CH_3)_2CO]_2\}_\infty$ (**2b**), and $\{p\text{-}C_6H_4[CH_2OCH_2C(pz)_3]_2AgPF_6\}_\infty$ (**3a**), where the stoichiometry for the latter compound has changed from a metal:ligand ratio of 2:1 to 1:1. The structure of **1a** is based on helical argentachains constructed by a κ^2–κ^1 coordination to silver of the tris(pyrazolyl)methane units. These chains are organized into a tubular 3D structure by cylindrical $[(CF_3SO_3)_6]^{6-}$ clusters that form weak C–H···O hydrogen bonds with the bitopic ligand. The same κ^2–κ^1 coordination is present in the structure of **2a**, but the structure is organized by six different tris(pyrazolyl)methane units from six ligands bonding with six silvers to form a 36-member argentamacrocycle core. The cores are organized in a tubular array by the organic spacers where each pair of macrocycles sandwich six acetone molecules and one SbF_6^- counterion. The structure of **3a** is based on a κ^2–κ^0 coordination mode of each tris(pyrazolyl)methane unit forming a helical coordination polymer, with two strands organized in a double stranded helical structure by a series of C–H···π interactions between the central arene rings. Crystallization of **2**–**4** from acetonitrile yields complexes of the formula $\{p\text{-}C_6H_4[CH_2OCH_2C(pz)_3]_2[(AgX)_2(CH_3CN)_n]\}_\infty$ where $n = 2$ for X = SbF_6^- (**2b**), X = PF_6^- (**3b**) and $n = 1$ for X = BF_4^- (**4b**). All three structures contain argentachains formed by a κ^2–κ^1 coordination mode of the tris(pyrazolyl)methane units linked by the organic spacer and arranged in a 2D sheet structure with the anions sandwiched between the sheets. Crystallization of **5** from acetonitrile yields crystals of the formula $\{p\text{-}C_6H_4[CH_2OCH_2C(pz)_3]_2(AgNO_3)_2(CH_3CN)_4\}_\infty$, where the nitrate is bonded to the silver. The argentachains, again formed by κ^2–κ^1 coordination, are arranged in W-shaped sheets that have an overall configuration very different from **2b**–**4b**. Treating $\{p\text{-}C_6H_4[CH_2OCH_2C(pz)_3]_2(AgSbF_6)_2\}_\infty$ with a saturated aqueous solution of KPF_6 or KO_3SCF_3 slowly leads to complete exchange of the anion. Crystallization of a sample that contains an approximately equal mixture of SbF_6^-/PF_6^- from acetonitrile yields $\{p\text{-}C_6H_4[CH_2OCH_2C(pz)_3]_2[Ag_2(PF_6)_{0.78(1)}(SbF_6)_{1.22(1)}(CH_3CN)_2][(CH_3CN)_{0.25}\ (C_4H_{10}O)_{0.25}]\}_\infty$, a compound with a sheet structure analogous to **2b**–**4b**. Crystallization of the same mixture from acetone yields $\{p\text{-}C_6H_4[CH_2OCH_2C(pz)_3]_2(AgSbF_6)[(CH_3)_2CO]_{1.5}\}_\infty$, where the metal-to-ligand ratio is 1:1 and the $[C(pz)_3]$ units are κ^2–κ^0 bonded forming a coordination polymer. The supramolecular structures of all species are organized by a combination of C–H···π, π–π, or weak C–H–F(O) hydrogen bonding interactions.

Introduction

The key features that determine the overall architectures of self-assembled species are the nature of coordinating groups, the ligand topicity (i.e., the number and position of coordinating groups), flexibility or rigidity of the linker groups joining the coordination sites, and the stereochemical preferences of the coordinated metal ion.[1–3] The role of noncovalent interactions is also recognized as providing further organization into more complex networks. A wide

* To whom correspondence should be addressed. E-mail: Reger@mail.chem.sc.edu.

10.1021/ic035207i CCC: $27.50
Published on Web 12/30/2003

variety of these interactions, some relating to the anions[3a−d,4] and the solvent,[2g,3b,5] have been found to impact the organization of such compounds. Important examples are strong[5] and weak[3e,7] hydrogen bonds, $\pi-\pi$ stacking,[8] X−H···π interactions (X = O, N, C),[9] and interhalogen interactions.[10] Silver(I) is frequently used as the metal because the flexibility of its coordination sphere can produce sophisticated coordination architectures. This flexibility affords an opportunity to investigate how the self-assembly process is influenced by modifications of the ligand denticity, the ligand-to-metal ratio, the counterions, and noncovalent interactions.[3a−d,4−10,11]

Insight into the self-assembly process can be obtained by carrying out systematic studies using a series of similar complexes assembled from a specific ligand and the same metallic center and imposing subtle alterations in the environment such as changing the anions and the crystallization solvent. Extensive research has been done in this area using mostly rigid ligands because they allow a better prediction of the overall structure, shape, and porosity of the resulting array. Schröder et al., studying silver(I) coordination polymers based on aromatic nitrogen-donor ligands, found, besides covalent metal−ligand contacts, that a plethora of interactions (e.g., $\pi-\pi$ interactions, metal−metal interactions, metal−π interactions) have an influence on the outcome of the resulting supramolecular array.[1c,d,11c] Zaworotko,[12] Yaghi,[13] and others[14] used polycarboxylic acids and various metal centers to construct both discrete and infinite architectures, based on the rigid orientation and binding mode of the ligand to the metallic centers. All these studies gave rise to a series of principles that can be applied in the design of new structures with a high degree of confidence.

At the opposite end of the spectrum are completely flexible ligands. Ciani et al.[15] used various flexible ligands and investigated the effect of the counterions and the length of the chain on the coordination networks formed by these

(1) (a) Piguet, C.; Bernardinelli, G.; Hopfgartner G. *Chem. Rev.* **1997**, *97*, 2005. (b) Hagrman, P. J.; Hagrman, D.; Zubieta, J. *Angew. Chem., Int. Ed*. **1999**, *38*, 2638. (c) Khlobystov, A. N.; Blake, A. J.; Champness, N. R.; Lemenovskii, D. A.; Majouga, G.; Zyk, N. V.; Schroder, M. *Coord. Chem. Rev.* **2001**, *222*, 155. (d) Blake, A. J.; Champness, N. R.; Hubberstey, P.; Li, W. S.; Withersby, M. A.; Schroder, M. *Coord Chem. Rev.* **1999**, *183*, 117. (e) Batten, S. T.; Robson, R. *Angew. Chem., Int. Ed.* **1998**, *37*, 1461. (f) Nguyen, P.; Gomez-Elipe, P.; Manners, I. *Chem. Rev.* **1999**, *99*, 1515. (g) Leininger, S.; Olenyuk, B.; Stang, P. J. *Chem. Rev.* **2000**, *100*, 853. (h) Swiegers, G. F.; Malefetse, T. J. *Chem. Rev*. **2000**, *100*, 3483. (i) Seidel, R. S.; Stang, P. J. *Acc. Chem. Res*. **2002**, *35*, 972. (j) Zaworotko, M. J. *Chem. Commun*. **2001**, 1. (k) Carlucci, L.; Ciani, G.; Proserpio, D. M. *CrystEngComm* **2003**, *5*, 269. (l) Siemeling, U.; Scheppelmann, I.; Neumann, B.; Stammler, A.; Stammler, H.-G.; Frelek, J. *Chem. Commun*. **2003**, 2236. (m) Burchell, T. J.; Eisler, D. J.; Jennings, M. C.; Puddephatt, R. J. *Chem. Commun.* **2003**, 2228. (n) Dong, Y.-B.; Cheng, J.-Y.; Huang, R.-Q.; Smith, M. D.; Zur Loye, H.-C. *Inorg. Chem.* **2003**, *42*, 5699. (o) Albrecht, M. *Chem. Rev.* **2001**, *101*, 3457.

(2) (a) Gardner, G. B.; Venkataraman, D.; Moore, J. S.; Lee, S. *Nature* **1995**, *374*, 792. (b) Venkataraman, D.; Gardner, G. B.; Lee, S.; Moore J. S. *J. Am. Chem. Soc.* **1995**, *117*, 11600. (c) Yaghi, O. M.; Li, G.; Li, H. *Nature* **1995**, *378*, 703. (d) Hennigar, T. J.; MacQuarrie, D. C.; Losier, P.; Rogers, R. D.; Zaworotko, M. J. *Angew. Chem., Int. Ed.* **1997**, *36*, 972. (e) Müller, I. M.; Röttgers, T.; Sheldrik, W. S. *Chem. Commun*. **1998**, 823. (f) Hong, M.; Zhao, Y.; Su, W.; Cao, R.; Fujita, M.; Zhou, Z.; Chan, A. S. C. *Angew. Chem., Int. Ed.* **2000**, *39*, 2468. (g) Blake, A. J.; Champness, N. R.; Cooke, P. A.; Nicolson, J. E. B. *Chem. Commun.* **2000**, 665.

(3) (a) Hirsch, K. A.; Wilson, S. R.; Moore, J. S. *Inorg. Chem*. **1997**, *36*, 2960. (b) Blake, A. J.; Champness, N. R.; Cooke, P. A.; Nicolson, J. E. B.; Wilson, C. *J. Chem. Soc., Dalton Trans*. **2000**, 3811. (c) Yang, S.-P.; Chen, X.-M.; Ji, L. *J. Chem. Soc., Dalton Trans*. **2000**, 2337. (d) Fei, B.-L.; Sun, W.-Y.; Yu, K-.B.; Tang, W.-X. *J. Chem. Soc., Dalton Trans*. **2000**, 805. (e) Paul, R. L.; Couchman, S. M.; Jeffery, J. C.; McCleverty, J. A.; Reeves, Z. R.; Ward, M. D. *J. Chem. Soc., Dalton Trans.* **2000**, 845. (f) Carlucci, L.; Ciani, G.; Proserpio, D. M.; Rizzato, S. *CrystEngComm* **2002**, *4*, 121. (g) Plater, J. M.; Foreman, M. R. St. J.; Slawin, A. M. *J. Chem. Res., Synop*. **1999**, 74. (h) Carlucci, L.; Ciani, G.; Proserpio, D. M.; Rizzato, S. *CrystEngComm* **2002**, *4*, 431.

(4) (a) Withersby, M. A.; Blake, A. J.; Champness, N. R.; Hubberstey, P.; Li W.-S.; Schröder, M. *Angew. Chem., Int. Ed.* **1997**, *36*, 2327. (b) Vilar, R.; Mingos, D. M. P.; White, A. J. P.; Williams, D. J. *Angew. Chem., Int. Ed*. **1998**, *37*, 1258. (c) Hong, M. C.; Su, W. P.; Cao, R.; Fujita, M.; Lu, J. X. *Chem. Eur. J.* **2000**, *6*, 427.

(5) (a) Withersby, M. A.; Blake, A. J.; Champness, N. R.; Cooke, P. A.; Hubberstey, P.; Li, W.-S.; Schröder, M. *Inorg. Chem.* **1999**, *38*, 2259. (b) Subramanian, S.; Zaworotko, M. J. *Angew. Chem., Int. Ed.* **1995**, *34*, 2127. (c) Lu, J.; T. Paliwala, T.; Lim, S. C.; Yu, C.; Niu, T.; Jacobson, A. J. *Inorg. Chem.* **1997**, *36*, 923.

(6) Strong hydrogen bonds include interactions of the type O−H···O, N−H···O, O−H···N, and N−H···N. See for example: (a) Braga, D.; Grepioni, F. *J. Chem. Soc., Dalton Trans*. **1999**, 1. (b) Allen, M. T.; Burrows, A. D.; Mahon, M. F. *J. Chem. Soc., Dalton Trans*. **1999**, 215. (c) Ziener, U.; Breuning, E.; Lehn, J.-M.; Wegelius, E.; Rissanen, K.; Baum, G.; Fenske, D.; Vaughan, G. *Chem. Eur. J*. **2000**, *6*, 4132. (d) Goddard, R.; Claramunt, R. M.; Escolastico, C.; Elguero, J. *New. J. Chem.* **1999**, *23*, 237.

(7) Weak hydrogen bond (X−H···Y) involves less electronegative atoms; we discuss here only C−H···Y type of weak hydrogen bond (Y = O, F). See for example: (a) Calhorda, M. J. *Chem. Commun*. **2000**, 801. (b) Desiraju, G. R. *Acc. Chem. Res.* **1996**, *29*, 441. (c) Grepioni, F.; Cojazzi, G.; Draper, S. M.; Scully, N.; Braga, D. *Organometallics* **1998**, *17*, 296. (d) Weiss, H. C.; Boese, R.; Smith, H. L.; Haley, M. M. *Chem. Commun*. **1997**, 2403.

(8) (a) Hunter, C. A.; Sanders, J. K. M. *J. Am. Chem. Soc.* **1990**, *120*, 5525. (b) Janiak, C. *J. Chem. Soc., Dalton Trans*. **2000**, 3885 and references therein.

(9) (a) Takahashi, H.; Tsuboyama, S.; Umezawa, Y.; Honda, K.; Nishio, M. *Tetrahedron* **2000**, *56*, 6185. (b) Tsuzuki, S.; Honda, K.; Uchimaru, T.; Mikami, M.; Tanabe, K. *J. Am. Chem. Soc.* **2000**, *122*, 11450. (c) Seneque, O.; Giorgi, M.; Reinaud, O. *Chem. Commun*. **2001**, 984. (d) Weiss, H. C.; Blaser, D.; Boese, R.; Doughan, B. M.; Haley, M. M. *Chem. Commun*. **1997**, 1703. (e) Madhavi, N. N. L.; Katz, A. K.; Carrell, H. L.; Nangia, A.; Desiraju, G. R. *Chem. Commun*. **1997**, 2249. (f) Madhavi, N. N. L.; Katz, A. K.; Carrell, H. L.; Nangia, A.; Desiraju, G. R. *Chem. Commun*. **1997**, 1953. (g) Nishio, M.; Hirota, M.; Umezawa, Y. *The CH/π Interaction Evidence, Nature and Consequences*; Wiley-VCH: New York, 1998. (h) Jennings, W. B.; Farrell, B. M.; Malone, J. F. *Acc. Chem. Res.* **2001**, *34*, 885.

(10) (a) Reddy, D. S.; Craig, D. C.; Desiraju, G. R. *J. Am. Chem. Soc.* **1996**, *118*, 4090. (b) Kowalik, J.; VanDerveer, D.; Clower, C.; Tolbert, L. M. *Chem. Commun.* **1999**, 2007. (c) Freytag, M.; Jones, P. G.; Ahrens, B.; Fischer, A. K. *New J. Chem*. **1999**, *23*, 1137. (d) Thaimattam, R.; Reddy, D. S.; Xue, F.; Mak, T. C. W.; Nangia, A.; Desiraju, G. R. *New J. Chem*. **1998**, *22*, 143. (e) Edwards, A. J.; Burke, N. J.; Dobson, C. M.; Prout, K.; Heyes, S. J. *J. Am. Chem. Soc.* **1995**, *117*, 4637. (f) Desiraju, G. R.; Parthasarathy, R. *J. Am. Chem. Soc.* **1989**, *111*, 8725. (g) Pedireddi, V. R.; Reddy, D. S.; Goud, B. S.; Craig, D. C.; Rae, A. D.; Desiraju, G. R. *J. Chem. Soc., Perkin Trans. 2* **1994**, 2353. (h) Ruthe, F.; duMont, W. W.; Jones, P. G. *Chem. Commun*. **1997**, 1947. (i) Tanaka, K.; Fujimoto, D.; Toda, F. *Tetrahedron Lett.* **2000**, *41*, 6095.

(11) (a) Toyota, S.; Woods, C. R.; Benaglia, M.; Haldimann, R.; Wärnmark, K.; Hardcastle, K.; Siegel, J. S. *Angew. Chem., Int. Ed.* **2001**, *40*, 751. (b) Hiraoka, S.; Yi, T.; Shiro, M.; Shionoya, M. *J. Am. Chem. Soc.* **2002**, *124*, 14510. (c) Blake, A. J.; Baum, G.; Champness, N. R.; Chung, S. S. M.; Cooke, P. A.; Fenske, D.; Khlobystov, A. N.; Lemenovskii, D. A.; Li, W.-S.; Schroder, M. *J. Chem. Soc., Dalton Trans*. **2000**, 4285.

(12) (a) Abourahma, H.; Bodwell, G. J.; Lu, J.; Moulton, B.; Pottie, I. R.; Bailey, W. R.; Zaworotko, M. J. *Cryst. Growth Des.* **2003**, *3*, 513. (b) Bourne, S. A.; Mondal, A.; Zaworotko, M. J. *Cryst. Eng.* **2001**, *4*, 25. (c) Moulton, B.; Zaworotko, M. J. *Chem. Rev.* **2001**, *101*, 1629. (d) Lu, J.; Moulton, B.; Zaworotko, M. J.; Bourne, S. A. *Chem. Commun*. **2001**, 861.

Scheme 1. The Ligand *p*-$C_6H_4[CH_2OCH_2C(pz)_3]_2$ (L) and Possible Noncovalent Interactions That the Ligand Can Promote To Support Supramolecular Structures[a]

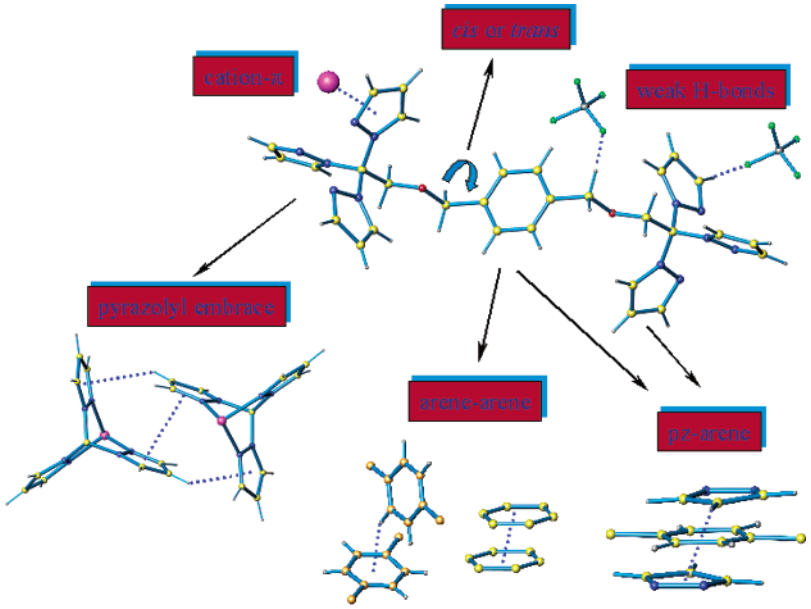

[a] Color code: metallic center, purple; carbon, yellow; oxygen, red; nitrogen, blue.

ligands and silver(I) salts. Several other research groups[16] also used flexible ligands in the construction of coordination polymers, and useful patterns with potential application in crystal engineering were found.[15,16]

The use of both types of ligands is, to some extent, restricted because rigid ligands limit the structures of possible products and flexible ligands have a very low degree of prediction of the resulting structure. At the interface between rigid and flexible ligands resides a class of ligands that contain in their structure both rigid and flexible parts and are designated as either "semirigid" or "semiflexible" ligands or sometimes "flexible" only, although they have the same features.[17]

We are investigating the field of coordination polymers using a new class of semirigid ligands based on linking two or more tris(pyrazol-1-yl)methane units in a single molecule.[18] The chemistry reported here is based on the bitopic ligand *p*-$C_6H_4[CH_2OCH_2C(pz)_3]_2$ (**L**, pz = pyrazolyl ring), shown in Scheme 1. Also shown are the noncovalent interactions and/or conformations that are possible with this ligand. The ether linkage offers the possibility of *cis* or *trans* orientations of the sidearms, while the presence of acidic hydrogen atoms on the pyrazolyl ring or the methylene groups adjacent to oxygen on the sidearms can promote weak hydrogen bonds if suitable proton acceptors are introduced into the system.[18a,b,d,h] The presence of aromatic pyrazolyl rings and linking arene ring that can act as acceptors in

(13) (a) Yaghi, O. M.; O'Keeffe, M.; Ockwig, N. W.; Chae, H. K.; Eddaoudi, M.; Kim, J. *Nature* **2003**, *423*, 705. (b) Rosi, N. L.; Eckert, J.; Eddaoudi, M.; Vodak, D. T.; Kim, J.; O'Keeffe, M.; Yaghi, O. M. *Science* **2003**, *300*, 1127. (c) Rosi, N. L.; Eddaoudi, M.; Kim, J.; O'Keeffe, M.; Yaghi, O. M. *CrystEngComm* **2002**, *4*, 401. (d) Rosi, N. L.; Eddaoudi, M.; Kim, J.; O'Keeffe, M.; Yaghi, O. M. *Angew. Chem., Int. Ed.* **2002**, *41*, 284. (e) Braun, M. E.; Steffek, C. D.; Kim, J.; Rasmussen, P. G.; Yaghi, O. M. *Chem. Commun.* **2001**, 2532. (f) Eddaoudi, M.; Kim, J.; O'Keeffe, M.; Yaghi, O. M. *J. Am. Chem. Soc.* **2002**, *124*, 376. (g) Eddaoudi, M.; Moler, D. B.; Li, H.; Chen, B.; Reineke, T. M.; O'Keeffe, M.; Yaghi, O. M. *Acc. Chem. Res.* **2001**, *34*, 319. (h) Chen, B.; Eddaoudi, M.; Hyde, S. T.; O'Keeffe, M.; Yaghi, O. M. *Science* **2001**, *291*, 1021. (i) Chen, B.; Eddaoudi, M.; Reineke, T. M.; Kampf, J. W.; O'Keeffe, M.; Yaghi, O. M. *J. Am. Chem. Soc.* **2000**, *122*, 11559.

(14) (a) Wang, Y.; Cao, R.; Sun, D.; Bi, W.; Li, X.; Li, X. *J. Mol. Struct.* **2003**, *657*, 301. (b) Zhang, L.-P.; Mak, T. C. W. *Polyhedron* **2003**, *22*, 2787.

(15) (a) Carlucci, L.; Ciani, G.; Proserpio, D. M.; Rizzato, S. *Chem. Eur. J.* **2002**, *8*, 1519. (b) Carlucci, L.; Ciani, G.; Moret, M.; Proserpio, D. M.; Rizzato, S. *Chem. Mater.* **2002**, *14*, 12. (c) Carlucci, L.; Ciani, G.; Proserpio, D. M.; Rizzato, S. *Chem. Commun.* **2000**, 1319. (d) Carlucci, L.; Ciani, G.; v. Gundenberg, D. W.; Proserpio, D. M. *Inorg. Chem.* **1997**, *36*, 3812.

(16) (a) Ng, M. T.; Deivaraj, T. C.; Vittal, J. J. *Inorg. Chim. Acta* **2003**, *348*, 173. (b) Chen, C.-L.; Su, C.-Y.; Cai, Y.-P.; Zhang, H.-X.; Xu, A.-W.; Kang, B.-S. *New J. Chem.* **2003**, *27*, 790. (c) Gao, E.-Q.; Bai, S.-Q.; Wang, Z.-M.; Yan, C.-H. *J. Chem. Soc., Dalton Trans.* **2003**, 1759. (d) Erxleben, A. *CrystEngComm* **2002**, *4*, 472. (e) Tong, M.-L.; Wu, Y.-M.; Ru, J.; Chen, X.-M.; Chang, H.-C.; Kitagawa, S. *Inorg. Chem.* **2002**, *41*, 4846. (f) Bu, X.-H.; Chen, W.; Hou, W.-F.; Du, M.; Zhang, R.-H.; Brisse, F. *Inorg. Chem.* **2002**, *41*, 3477. (g) Brandys, M.-C.; Puddephatt, R. J. *J. Am. Chem. Soc.* **2002**, *124*, 3946. (h) Bu, X.-H.; Chen, W.; Lu, S.-L.; Zhang, R.-H.; Liao, D.-Z.; Bu, W.-M.; Shionoya, M.; Brisse, F.; Ribas, J. *Angew. Chem., Int. Ed.* **2001**, *40*, 3201. (i) McMorran, D. A.; Pfadenhauer, S.; Steel, P. J. *Aust. J. Chem.* **2002**, *55*, 519. (j) Tabellion, F. M.; Seidel, S. R.; Arif, A. M.; Stang, P. J. *J. Am. Chem. Soc.* **2001**, *123*, 11982. (k) Tabellion, F. M.; Seidel, S. R.; Arif, A. M.; Stang, P. J. *J. Am. Chem. Soc.* **2001**, *123*, 7440.

(17) (a) Kasai, K.; Aoyagi, M.; Fujita, M. *J. Am. Chem. Soc.* **2000**, *122*, 2140. (b) Seward, C.; Chan, J. L.; Song, D. T.; Wang, S. N. *Inorg. Chem.* **2003**, *42*, 1112. (c) Sun, D. F.; Cao, R.; Sun, Y. Q.; Bi, W. H.; Li, X. H.; Hong, M. C.; Zhao, Y. J. *Eur. J. Inorg. Chem.* **2003**, 38. (d) McMorran, D. A.; Pfadenhauer, S.; Steel, P. J. *Inorg. Chem. Commun.* **2002**, *5*, 449. (e) Banfi, S.; Carlucci, L.; Caruso, E.; Ciani, G.; Proserpio, D. M. *J. Chem. Soc., Dalton Trans.* **2002**, 2714. (f) Fujita, M.; Sasaki, O.; Watanabe, K.; Ogura, K.; Yamaguchi, K. *New J. Chem.* **1998**, *22*, 189.

(18) (a) Reger, D. L.; Wright, T. D.; Semeniuc, R. F.; Grattan, T. C.; Smith, M. D. *Inorg. Chem.* **2001**, *40*, 6212. (b) Reger, D. L.; Semeniuc, R. F.; Smith, M. D. *Inorg. Chem.* **2001**, *40*, 6545. (c) Reger, D. L.; Semeniuc, R. F.; Smith, M. D. *Eur J. Inorg. Chem.* **2002**, 543. (d) Reger, D. L.; Semeniuc, R. F.; Smith, M. D. *J. Chem. Soc., Dalton Trans.* **2002**, 476. (e) Reger, D. L.; Semeniuc, R. F.; Smith, M. D. *Inorg. Chem. Commun.* **2002**, *5*, 278. (f) Reger, D. L.; Semeniuc, R. F.; Smith, M. D. *J. Organomet. Chem.* **2003**, *666*, 87. (g) Reger, D. L.; Semeniuc, R. F.; Smith, M. D. *J. Chem. Soc., Dalton Trans.* **2003**, 285. (h) Reger, D. L.; Semeniuc, R. F.; Silghi-Dumitrescu, I.; Smith, M. D. *Inorg. Chem.* **2003**, *42*, 3751.

Scheme 2. Possible Modes of Coordination of Tris(pyrazolyl)methane Units

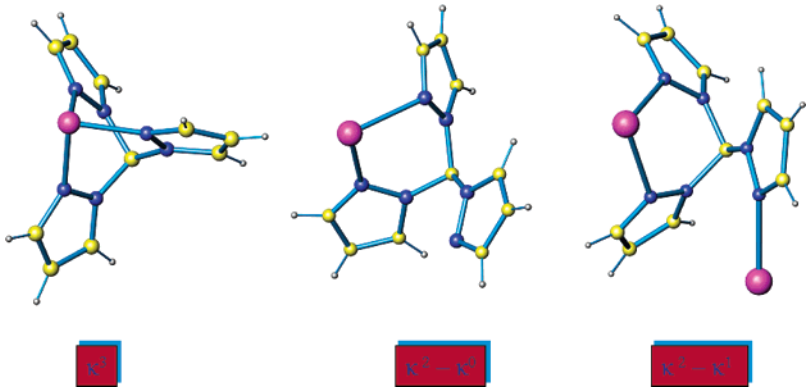

C−H···π interactions[18f−h] or participate in $\pi-\pi$ stacking[18,b,d,f,h] can lead to arene−arene, pyrazolyl−arene interactions or the double $\pi-\pi$ stacking/C−H···π interaction we have named, after a CSD database search showed that it was a general interaction, the "quadruple pyrazolyl embrace".[19] Another possible noncovalent interaction is cation−π interactions between a metallic center and a pyrazolyl ring within the ligand.[20] In addition, the tris(pyrazolyl)methane units can act in different binding modes as (a) κ^3 tripodal, (b) κ^2 bonded to a single metal with the third pyrazolyl not coordinated, and (c) $\kappa^2-\kappa^1$ bonded bridging two metals (Scheme 2). As a means of simplifying the language related to these types of semirigid ligands used in supramolecular chemistry, both those developed in our group and elsewhere, we define them as "structurally adaptive".

Reported here are the syntheses and characterization of a series of silver(I) coordination polymers of this versatile ligand. We have carefully investigated the supramolecular structural modifications influenced by several types of noncovalent forces when the anions and crystallization solvent are varied, with an emphasis on the solid-state structures. The solution structure and dynamics, as deduced from ^{1}H NMR and, indirectly, from ESI-MS, are also discussed. We have previously communicated the structures of three of these compounds.[18c,g]

Results and Discussion

Syntheses and Characterization. The bitopic ligand **L** was prepared[18a] in a one pot synthesis starting from α,α′-dibromo-*p*-xylene, *p*-$(BrCH_2)_2C_6H_4$, and tris-2,2,2-(1-pyrazolyl)ethanol, HO−CH_2−C$(pz)_3$, under basic (NaH) conditions. NMR and elemental analysis confirmed its chemical composition and purity. The preparation of the complexes was readily achieved by combining the ligand with the respective metal salts in a 2:1 metal-to-ligand ratio. The compounds (insoluble in halogenated solvents, water, or alcohols but soluble in acetone, acetonitrile, and nitromethane) are white solids that are air stable and show only slight decomposition after several weeks of exposure to daylight.

$$2n\mathrm{AgX} + n\{p\text{-}C_6H_4[CH_2OCH_2C(pz)_3]_2\} \xrightarrow{\mathrm{THF}} \{p\text{-}C_6H_4[CH_2OCH_2C(pz)_3]_2(\mathrm{AgX})_2\}n$$

X = $CF_3SO_3^-$ (**1**), SbF_6^- (**2**), PF_6^- (**3**), BF_4^- (**4**), and NO_3^- (**5**)

Elemental analyses of the solids correspond to a metal-to-ligand ratio of 2:1; therefore, the complexes are formulated as follows: $\{p\text{-}C_6H_4[CH_2OCH_2C(pz)_3]_2(\mathrm{AgX})_2\}_\infty$, where X = $CF_3SO_3^-$ (**1**), SbF_6^- (**2**), PF_6^- (**3**), BF_4^- (**4**), and NO_3^- (**5**). The same metal-to-ligand ratio was found when the starting materials were mixed in a 1:1 reaction, with half an equivalent of the ligand recovered from the filtrate. While the chemical composition of the products is by no means sufficient for making any structural predictions due to the many different structural architectures of coordination frameworks that can be generated from identical stoichiometries, we established[18a] by molecular mechanics calculations that the overall length and structure of the xylene based bridge prevent simultaneous coordination of both sides of **L** to one metal center.

The ^{1}H NMR spectra of the solids in CD_3CN show that the acetonitrile completely replaces the ligand; the spectrum of the compound in CD_3CN is the same as the free ligand in this solvent. However, the ^{1}H spectra of the compounds in deuterated acetone are clearly different from the free ligand, showing the coordination of the ligand to the silver(I) in solution. Although the X-ray structure shows that in the solid state the pyrazolyl rings are nonequivalent (vide infra), the NMR spectra show equivalent rings, presumably because of fast exchange of the ligands and metals on the NMR time scale. This fast exchange process is maintained even at low temperatures. The spectra of metal complexes **1**−**5** in acetone are essentially identical, showing the same upfield shifts when compared to the free ligand. This result suggests that the species present in acetone solution are identical and anion independent. Electrospray mass spectroscopy showed peaks corresponding to $[\mathbf{L}Ag]^+$ and $[\mathbf{L}Ag_2X]^+$ (except for **3** that only shows $[\mathbf{L}Ag]^+$). Surprisingly, these spectra were very similar when run in either acetone or acetonitrile.

(19) Reger, D. L.; Gardinier, J. R.; Semeniuc, R. F.; Smith, M. D. *J. Chem. Soc., Dalton Trans.* **2003**, 1712.

(20) For examples of cation−π interactions between metallic centers and pyrazolyl rings see: (a) Craven, E.; Mutlu, E.; Lundberg, D.; Temizdemir, S.; Dechert, S.; Brombacher, H.; Janiak, C. *Polyhedron* **2002**, *21*, 553. (b) Kisko, J. L.; Hascall, T.; Kimblin, C.; Parkin, G. *J. Chem. Soc., Dalton Trans.* **1999**, 1929. (c) Janiak, C.; Temizdemir, S.; Scharmann, T. G. *Z. Anorg. Allg. Chem.* **1998**, *624*, 755.

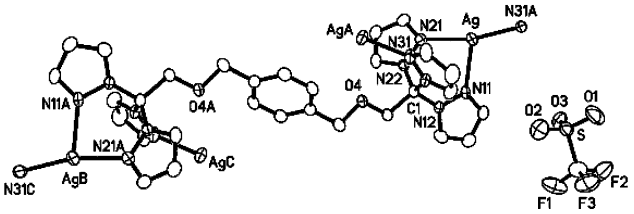

Figure 1. ORTEP representation of $\{p\text{-}C_6H_4[CH_2OCH_2C(pz)_3]_2(AgCF_3SO_3)_2\}_\infty$ (**1a**) with displacement ellipsoids shown at 50% probability level.

In order to ascertain the influences of the crystallization solvent and the counterion on the resulting "molecular" and supramolecular structures of the compounds, we performed crystallization procedures using acetone and acetonitrile as solvents and diethyl ether as precipitating agent, using the vapor phase diffusion method. All other conditions (ambient temperature, concentration of the mother liquors) were kept unchanged. In 7 of the 10 possible cases (**1a**, **2a**, **3a**, from acetone, and **2b**, **3b**, **4b**, **5**·4CH_3CN, from acetonitrile) crystals formed that were subjected to X-ray diffraction studies.

Solid-State Structures. In describing the highly organized supramolecular structures reported here, we will use the terminology developed by Lehn.[21] The primary structure of a supramolecular compound is created by the covalent bonds of the individual atoms in the reacting building blocks (also known as "tectons"[22]), with the secondary structure being the arrangement of the tectons one with respect to another. If one or more secondary structural elements impose a further distinct and more encompassing motif on the compound as a whole, this arrangement is the tertiary structure and constitutes the dominant structural motif. If several separate tertiary structural units are connected, the resulting compound would have four levels of structural organization, with quaternary structure required to describe the arrangement of the "individual" tertiary structural units relative to each other.

Crystallization of the product resulting from the reaction of $AgCF_3SO_3$ and $p\text{-}C_6H_4[CH_2OCH_2C(pz)_3]_2$ from acetone leads to the formation of $\{p\text{-}C_6H_4[CH_2OCH_2C(pz)_3]_2(AgCF_3SO_3)_2\}_\infty$ (**1a**), a compound with a metal/ligand ratio of 2:1. In the primary structure (Figure 1) the ligand has a skewed *trans* arrangement of the sidearms with respect to the central arene ring. Each tris(pyrazolyl)methane unit has a $\kappa^2-\kappa^1$ coordination to silver placing three nitrogen atoms around each metal in a distorted trigonal planar arrangement with the sum of the N−Ag−N angles being nearly 360°. The Ag−N bond distances and angles display no unusual features and are provided as Supporting Information.

The secondary structure consist of single stranded helical chains constructed by this $\kappa^2-\kappa^1$ coordination generating helical argentachains (no interactions between the silver(I) centers are implied), with a AgNNCNN sequence (Figure 2a), that are oriented along a crystallographic 3_1 screw axis. Figure 2b shows the view down two of the chiral chains.

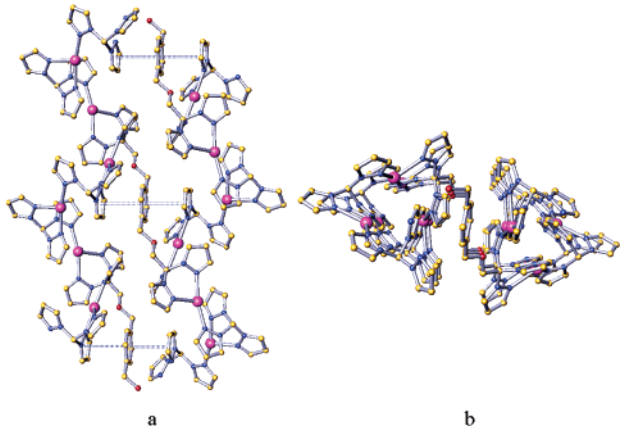

Figure 2. (a) Two adjacent helical argentachains for $\{p\text{-}C_6H_4[CH_2OCH_2C(pz)_3]_2(AgCF_3SO_3)_2\}_\infty$ (**1a**), showing the double $\pi-\pi$ stacking. (b) View of the same helical argentachains down the helical axis. Color code is the same as in Scheme 1, with silver = purple.

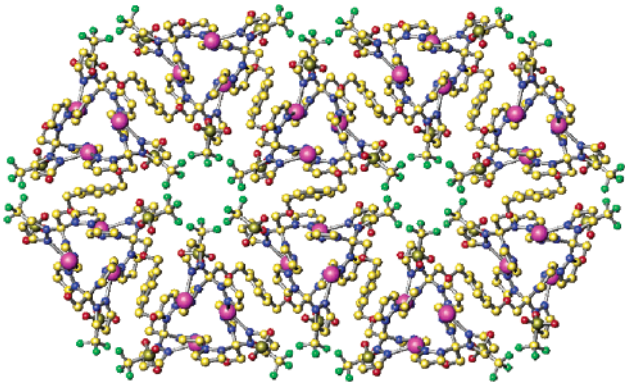

Figure 3. Overall structure of **1a**, down the *c* axis. Color code is the same as in Scheme 1, plus sulfur = light brown and fluorine = green.

These helical chains are organized in a tertiary structure by the ether-based sidearms combined with a double face-to-face $\pi-\pi$ stacking, involving two pyrazolyl rings sandwiching the central phenyl ring.[8] Figure 3 shows the overall 3D arrangement of **1a**. Six helical chains, connected by the organic bridges, are arranged in cylinders around a central core of triflate anions. Each adjacent cylinder shares a pair of helical chains such that each of the AgNNCNN helices is part of three overlapping cylinders. A schematic representation of the structure is illustrated in Figure 4. Every cylinder overlaps with six other cylinders, with every helical chain being surrounded by three helical chains of opposite chirality.

Noncovalent interactions from the triflate anions are clearly important in this arrangement of the 3D structure into "cylinders". The triflate anions in **1a** are not bonded to silver as in other cases[17b,23] but are arranged in circular clusters of six, the same as the number of helices in each cylinder. As shown in Figure 5, six S_6 symmetry related triflate anions

(21) Hasenknopf, B.; Lehn, J.-M.; Boumediene, N.; Dupont-Gervais, A.; van Dorsselaer, A.; Kneisel, B.; Fenske, D. *J. Am. Chem. Soc.* **1997**, *119*, 10956.

(22) Tecton = any molecule whose interactions are dominated by particular associative forces that induce self-assembly of an organized network with specific architectural or functional features. See: Simard, M.; Su, D.; Wuest, J. D. *J. Am. Chem. Soc.* **1991**, *113*, 4696.

(23) For examples of OTf^- coordinated to a silver(I) center in coordination polymers see: (a) Ino, I.; Wu, L. P.; Munakata, M.; Maekawa, M.; Suenaga, Y.; Kuroda-Sowa, T.; Kitamori, Y. *Inorg. Chem.* **2000**, *39*, 2146. (b) Venkataraman, D.; Lee, S.; Moore, J. S.; Zhang, P.; Hirsch, K. A.; Gardner, G. B.; Covey, A. C.; Prentice, C. L. *Chem. Mater.* **1996**, *8*, 2030. (c) Buchholz, H. A.; Prakash, G. K. S.; Vaughan, J. F. S.; Bau, R.; Olah, G. A.; *Inorg. Chem.* **1996**, *35*, 4076.

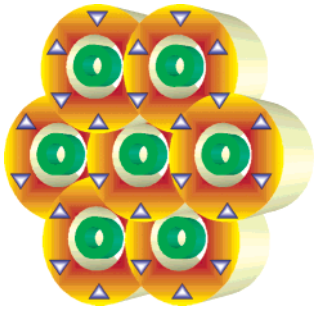

Figure 4. Schematic representation of **1a**: orange rings are cylinders of helical argentachains connected by the organic spacer; green rings are circular association of the triflate anions; blue triangles are 3_1 helical argentachains with "▲" and "▼" representing opposite handed helices.

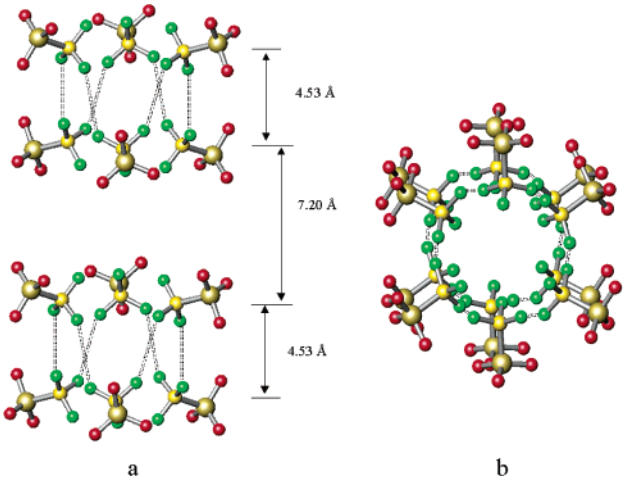

Figure 5. (a) Two triflate clusters of **1a**, view perpendicular to *c* axis, showing the distances (Å) between planes formed by the carbon atoms of triflate groups. (b) The same two triflate clusters, viewed end on.

have their fluorine atoms directed toward one another. The cluster is formed by the circular arrangement of three triflate anions in a plane and three others related by an S_6 symmetry operation. The distance between the planes formed by the carbon atoms of the triflate groups within the cluster is 4.53 Å. In contrast, the distance between two adjacent planes from two separate clusters is 7.20 Å.

Attractive interactions of the type X···X (X = F, Cl, Br, I) are known to play an important role in many structures, although the exact nature of the interaction is still unclear.[10] For compound **1a**, the shortest F···F distances are 3.28 Å, more than the sum of the van der Waals radii for fluorine at 2.94 Å.[24] The energy of interaction between the fluorine atoms of the triflate groups at 3.28 Å in the $[(CF_3SO_3)_6]^{6-}$ clusters was calculated on the MP2/aug-cc-pVDZ level of theory, with only the valence electrons correlated. The calculation was based on the work of Halkier et al.[25] and on the experimentally measured shortest F···F distance. We neglected the basis set superposition error and presume our basis set to be sufficiently large for a qualitatively correct estimate. The energy of interaction between two adjacent fluorine atoms at the Hartree−Fock level is 0.34 kcal/mol.

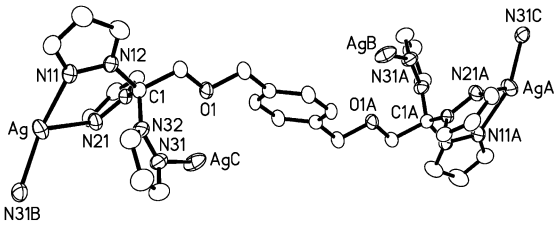

Figure 6. ORTEP representation of the cationic unit in $\{p\text{-}C_6H_4[CH_2OCH_2C(pz)_3]_2(AgSbF_6)_2[(CH_3)_2CO]_2\}_\infty$ (**2a**) with displacement ellipsoids shown at 40% probability level.

The Hartree−Fock model does not describe van der Waals interactions. When these are included at the MP2 level, the energy of interaction between two adjacent fluorine atoms becomes 1.05 kcal/mol, making the F···F energy of interaction for each $[(CF_3SO_3)_6]^{6-}$ cluster 6.3 kcal/mol. This is a surprisingly large number, given the distance between the fluorines. We also calculated the energy of the F···F interaction in the one other example of a similar $(CF_3SO_3)_6^{6-}$ reported cluster.[26] In this case, the F···F distances are much shorter, in the range 2.7−2.9 Å. At this shorter distance, the average energy of each interaction increases to 1.93 kcal/mol, making the energy of interaction for each $(CF_3SO_3)_6^{6-}$ cluster 11.6 kcal/mol.

The hexameric triflate clusters control the circular arrangement of **2a** through the six SO_3^- groups that are oriented away from the center of the cluster. Each SO_3^- group makes two weak C−H···O hydrogen bonds with the bitopic ligand with metrical parameters that indicate both of these interactions are substantial. The presence of the hydrogen bonds is also supported by vibrational data of the trifluoromethanesulfonate anion by a 24 cm^{-1} blue-shift of the $\nu_{as}(E)$ stretching vibrations of the CF_3 group.[27]

The crystallization of the product resulting from the reaction of $AgSbF_6$ and $p\text{-}C_6H_4[CH_2OCH_2C(pz)_3]_2$ from acetone leads to the formation of $\{p\text{-}C_6H_4[CH_2OCH_2C(pz)_3]_2(AgSbF_6)_2[(CH_3)_2CO]_2\}_\infty$ (**2b**), a compound with the same metal/ligand ratio of 2:1 as in **1a**. Single crystal X-ray analysis showed that in **2a** the primary structure (Figure 6) is similar to that of **1a**, although the coordination environment around the silver(I) is more pyramidal, with the sum of the N−Ag−N angles being 341.71°.

However, the secondary structure of **2a** is very different from that of **1a**, although the same method of construction is used in the organization. As in **1a** each tris(pyrazolyl)-methane unit is κ^2 bonded to one silver(I) atom and κ^1 to another, but this construction does not lead to the formation of argentachains. Six $\kappa^2-\kappa^1$ $[C(pz)_3]$ units from six different ligands together with six silver atoms to form a 36-member argentamacrocycle core with the same AgNNCNN sequence as in the helical chain secondary structure of **1**, Figure 7. The shortest Ag···Ag distance is 5.54 Å indicating that there are no interactions between the silver(I) cations.

(24) (a) Bondi, A. *J. Phys. Chem.* **1964**, *68*, 441. (b) Rowland, R. S.; Taylor, R. *J. Phys. Chem.* **1996**, *100*, 738.
(25) Halkier, A.; Klopper, W.; Helgaker, T.; Jorgensen, P.; Taylor, P. R. *J. Chem. Phys.* **1999**, *111*, 9157.
(26) Su, C.-Y.; Kang, B.-S.; Wang, Q.-G.; Mak, T. C. W. *J. Chem. Soc., Dalton Trans.* **2000**, 1831.
(27) (a) Johnston, D. H.; Shriver, D. F. *Inorg. Chem.* **1993**, *32*, 1045. (b) Huang, W.; Wheeler, R. A.; Frech, R. *Spectrochim. Acta, Part A* **1994**, *50A*, 985. (c) Rhodes, C. P.; Frech, R. *Solid State Ionics* **2000**, *136−137*, 1131. (d) Huang, W.; Frech, R.; Wheeler, R. A. *J. Phys. Chem.* **1994**, *98*, 100. (e) Lawrance, G. F. *Chem. Rev.* **1986**, *86*, 17.

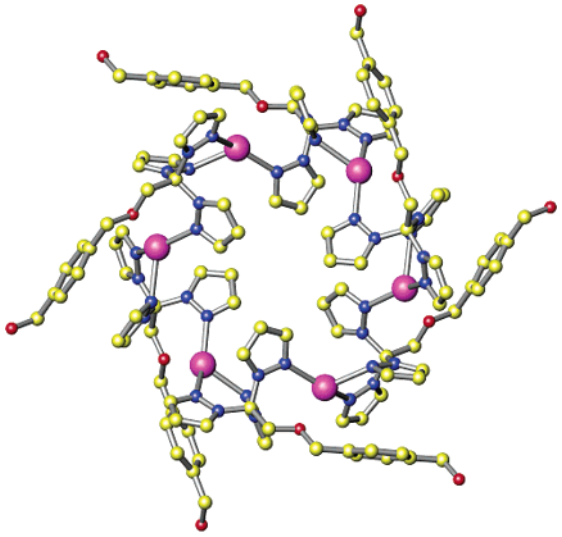

Figure 7. The argentamacrocycle core of $\{p\text{-}C_6H_4[CH_2OCH_2C(pz)_3]_2\text{-}(AgSbF_6)_2[(CH_3)_2CO]_2\}_\infty$ (**2a**) created by the $\kappa^2-\kappa^1$ bonding mode of the tris(pyrazolyl)methane units; hydrogen atoms omitted.

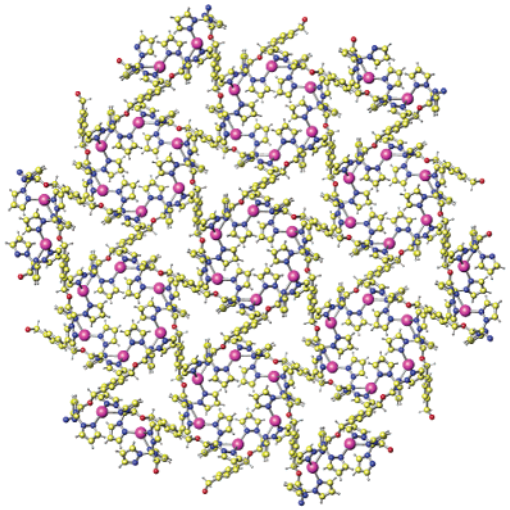

Figure 8. The overall structure of **2a**, SbF_6^- anions not shown, viewed down seven of the argentamacrocycle tubes connected by trigonally shaped helical spirals.

In the tertiary structure, the organic spacers that connect two $[C(pz)_3]$ units in the ligand link the argentamacrocycles in an extended tubular 3D structure. The ether-based sidearms have a skewed *trans* arrangement with the angle formed by the arene ring and the plane of the attached CH_2OCH_2 group of 42.6°. This orientation of the spacer allows a helical arrangement of the L−Ag−L−Ag sequence along a crystallographic 3_1 screw axis. Also supporting this structure is a double $\pi-\pi$ interaction involving the central arene core and two (symmetry related) pyrazolyl rings sandwiching the former aromatic moiety.[8b]

In the 3D tertiary structure, each argentamacrocycle is surrounded by six trigonally shaped helical spirals formed by the organic spacers that connect them to six other argentamacrocycles, Figure 8. A schematic representation of this arrangement that shows the relative position of the macrocycles is shown in Figure 9. Each helical spiral places every fourth argentamacrocycle on top of each other forming a tubular structure.

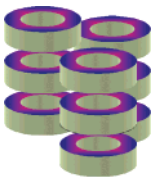

Figure 9. Schematic representation of the spatial arrangement of the argentamacrocycles showing the formation of the tubes in **2a**.

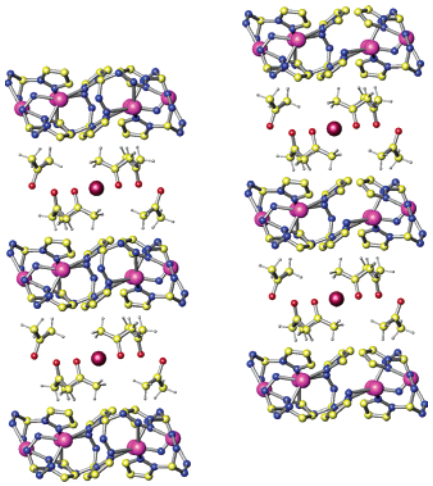

Figure 10. Six argentacrown cores, 24 acetone molecules, and four SbF_6^- anions building up two adjacent tubular metallamacrocycles in **2a** and their relative position one to another. Only essential atoms are shown, and the disordered fluorine atoms of the SbF_6^- groups are omitted.

Figure 10 shows the arrangement of two stacks of the argentamacrocycles that make up the tubes. Each pair of macrocycles sandwich six acetone molecules and one SbF_6^- counterion. The acetones interact with the argentamacrocycle cores via short C−H···π interactions with the pyrazolyl rings.[9] The location of the one SbF_6^- anion among the electron rich acetone double bonds and the π clouds from the pyrazolyl rings seems unusual. The remaining SbF_6^- anions are located in the chiral, helical channels of the spacers. Figure 10 shows that each argentamacrocycle "looks" like a crown and each pair acts as a "host" to a SbF_6^- and six acetone "guests".

Crystallization from acetone of the product from the reaction between $AgPF_6$ and $p\text{-}C_6H_4[CH_2OCH_2C(pz)_3]_2$ leads to the formation of $\{p\text{-}C_6H_4[CH_2OCH_2C(pz)_3]_2AgPF_6\}_\infty$ (**3a**). In contrast to **1a** and **2a** and the stoichiometry of the solid taken into the crystallization step, the metal/ligand ratio is 1:1. The primary structure consists (Figure 11) of two tris-(pyrazolyl)methane units bonded to silver(I) in a $\kappa^2-\kappa^0$ coordination mode. The silver atom has a tetrahedral environment, with a distortion imposed by the restricted "bite" angle of the chelating pyrazolyl rings (see bond distances and angles in Supporting Information). Each tris-(pyrazolyl)methane unit has one noncoordinated pyrazolyl ring. In the chain structure the ligand exists in an alternating *cis* and *trans* conformation, both pictured at the top of Figure 12. These conformers, combined with the κ^2-coordination mode, leads to a single stranded helical secondary structure, also shown in Figure 12. The presence of the cis ligand is critical to the helical organization of **3a**. Two single stranded helices of opposite chirality self-assemble in a tertiary

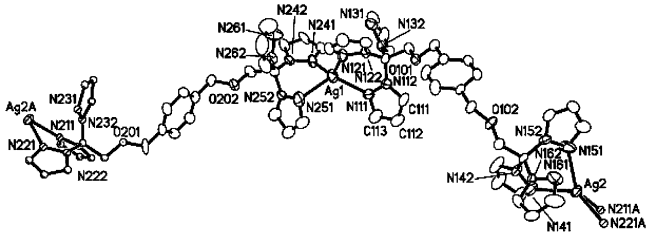

Figure 11. ORTEP representation of the strand repeat unit in **3a**. Individual strands in the double helix are related to one another by pure translation along the *a* axis; the double helix direction is along the *a* axis. Displacement parameters for atoms refined anisotropically shown at the 40% probability level and isotropic atoms drawn as spheres of arbitrary radii.

structure consisting of two strands wrapped one around another, leading to a double stranded helical structure, Figure 13. The "glue" that holds the helices together in the double stranded helix is a series of C−H···π interactions between the central arene rings, with the arene rings from the *cis* conformers acting as acceptors and with the arene rings from the *trans* conformers acting as donors. The H···centroid distance is 2.59 Å, with the corresponding C···centroid distance of 3.46 Å and the associated C−H···centroid angle of 153.4°. The counterions are not involved in any noncovalent interactions as reported in other cases for this anion,[7c,28] the crystal packing of the double stranded helices being based solely on van der Waals forces.

It should be noted that **3a** represents a rare example of a double stranded helical organization of a coordination polymer consisting of two separate single stranded helical chains wrapped one around another. In most of the known examples of discrete or infinite helical architectures, all the strands of the helix are attached through coordinate covalent bonds to the metal atoms that form the axis of the helix.[29] In contrast, there are only a few examples of chemical species that consist of single stranded helical independent chains interacting through one or another only by noncovalent interaction, with the resulting structure being a double helix.[30]

When acetone was replaced by acetonitrile in the crystallization procedure for compound **2**, crystals of the formula $\{p\text{-}C_6H_4[CH_2OCH_2C(pz)_3]_2[(AgSbF_6)_2(CH_3CN)_2][(CH_3CN)_{0.25}(C_4H_{10}O)_{0.25}]\}_\infty$ (**2b**) were obtained. Crystallographic studies revealed that the asymmetric unit contains two crystallographically nonequivalent Ag atoms and two independent SbF_6^- anions; two ligands are situated about crystallographic inversion centers, and therefore, only half of each ligand is present in the asymmetric unit (Figure 14). The primary structure is formed by the $\kappa^2-\kappa^1$ coordination mode of the tris(pyrazolyl)methane units. All silver atoms have a distorted tetrahedral environment, with an acetonitrile molecule occupying the fourth coordination site (Figures 14 and 15). The secondary structure is organized in argentachains, with the AgNNCNN sequence of construction, analogous to **1a** rather than the argentamacrocycles observed for **2a**. The chains are linked by the organic spacer (*trans* arrangement of the sidearms) and arranged in a 2D sheet tertiary structure. Figure 16 shows two such sheets oriented horizontally, down the argentachains showing the linking organic spacers, with the sheets sandwiching the SbF_6^- anions and disordered solvent molecules. The sheets are connected in a quaternary structure by means of hydrogen bonds between the SbF_6^- anions and acidic hydrogen atoms from the ligands, Figure 16. The H···F distances range from 2.24 to 2.38 Å and the C−H···F angles from 166.9° to 157.4°, values that suggest strong interactions within this class of weak noncovalent contacts.[7]

While the primary driving forces for this structure are the covalent bonds between the ligand, silver, and coordinated acetonitrile, the structure is also supported by an additional important noncovalent interaction, a C−H···π interaction between a hydrogen atom from a pyrazolyl ring that chelates the Ag(1) and the π system of the central arene ring. Interestingly, only one of the two nonequivalent central arene rings is involved in this interaction; the other one is not involved in any type of noncovalent interaction. Thus, as shown in Figure 15, every other row of central arene rings acts as an acceptor for two H(13) hydrogen atoms that sandwich the ring. This interaction arranges the argentachains in a flattened zigzag orientation within the overall sheet, as it can be seen in Figure 16.

Crystallization of **3** from acetonitrile yields crystals of the formula $\{p\text{-}C_6H_4[CH_2OCH_2C(pz)_3]_2[(AgPF_6)_2(CH_3CN)_2][(CH_3CN)_{0.25}(C_4H_{10}O)_{0.25}]\}_\infty$ (**3b**), a compound with a metal/ligand ratio of 2:1, in contrast to the 1:1 ratio found in **3a**. The structure is organized in the same manner with that of **2b**: a $\kappa^2-\kappa^1$ bonding mode of the tris(pyrazolyl)methane unit with a *trans* orientation of the ligand (Figure 17), leading to a sheet structure for **3b** similar to that depicted in Figures 14−16 for **2b**. However, a close analysis of the noncovalent interactions present in **3b** shows two major differences. First, although the sheet structure is supported by C−H···π interactions as in **2b**, in this case the central arene ring is the proton donor and a pyrazolyl ring is the acceptor. As in **2b**, every other row of central arene rings is involved in such an interaction, pictured in Figure 18. The second difference is that the PF_6^- anions are not involved in weak C−H···F

(28) (a) Cantrill, S. J.; Preece, J. A.; Stoddart, J. F.; Wang, Z.-H.; White, A. J. P.; Williams, D. J. *Tetrahedron* **2000**, *56*, 6675.

(29) For reviews on helical assemblies based on dative bonds see ref 1a and 1o; for selected recent examples see: (a) Wang, X.; Vittal, J. J. *Inorg. Chem. Commun*. **2003**, *6*, 1074. (b) Koeller, S.; Bernardinelli, G.; Piguet, C. *J. Chem. Soc., Dalton Trans*. **2003**, 2395. (c) Tuna, F.; Hamblin, J.; Jackson, A.; Clarkson, G.; Alcock, N. W.; Hannon, M. J. *J. Chem. Soc., Dalton Trans.* **2003**, 2141. (d) Khlobystov, A. N.; Brett, M. T.; Blake, A. J.; Champness, N. R.; Gill, P. M. W.; O'Neill, D. P.; Teat, S. J.; Wilson, C.; Schroeder, M. *J. Am. Chem. Soc.* **2003**, *125*, 6753. (e) Floquet, S.; Ouali, N.; Bocquet, B.; Bernardinelli, G.; Imbert, D.; Bunzli, J.-C. G.; Hopfgartner, G.; Piguet, C. *Chem. Eur. J.* **2003**, *9*, 1860. (f) Carlucci, L.; Ciani, G.; Proserpio, D. M.; Rizzato, S. *New J. Chem.* **2003**, *27*, 483. (g) Barboiu, M.; Vaughan, G.; Kyritsakas, N.; Lehn, J.-M. *Chem. Eur. J.* **2003**, *9*, 763. (h) Shova, S.; Novitchi, G.; Gdaniec, M.; Caneschi, A.; Gatteschi, D.; Korobchenko, L.; Voronkova, V. K.; Simonov, Y. A.; Turta, C. *Eur. J. Inorg. Chem*. **2002**, 3313. (i) Beauchamp, D. A.; Loeb, S. J. *Chem. Commun.* **2002**, 2484. (j) Keegan, J.; Kruger, P. E.; Nieuwenhuyzen, M.; Martin, N. *Cryst. Growth Des.* **2002**, *2*, 329. (k) Isola, M.; Liuzzo, V.; Marchetti, F.; Raffaelli, A. *Eur. J. Inorg. Chem*. **2002**, 1588. (l) Stahl, J.; Bohling, J. C.; Bauer, E. B.; Peters, T. B.; Mohr, W.; Martin-Alvarez, J. M.; Hampel, F.; Gladysz, J. A. *Angew. Chem., Int. Ed.* **2002**, *41*, 1871. (m) Albrecht, M.; Schneider, M. *Eur. J. Inorg. Chem.* **2002**, 1301. (n) Guo, D.; He, C.; Duan, C.-Y.; Qian, C.-Q.; Meng, Q.-J. *New J. Chem.* **2002**, *26*, 796.

(30) Selected examples: (a) Jouaiti, A.; Hosseini, M. W.; Kyritsakas, N. *Chem. Commun*. **2003**, 472. (b) Chen, X.-M.; Liu, G.-F. *Chem. Eur. J.* **2002**, *8*, 4811. (c) Mamula, O.; von Zelewsky, A.; Bark, T.; Bernardinelli, G. *Angew. Chem., Int. Ed.* **1999**, *38*, 2945.

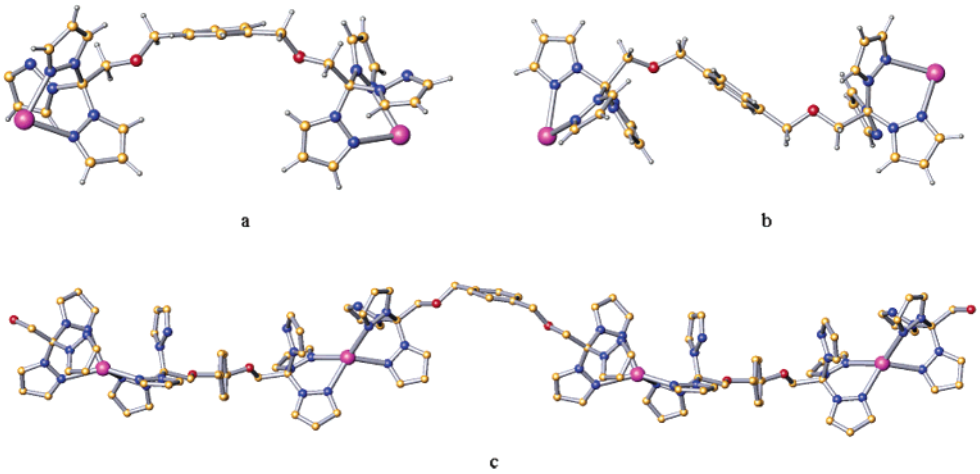

Figure 12. The formation of one helical single strand in $\{p\text{-}C_6H_4[CH_2OCH_2C(pz)_3]_2AgPF_6\}_\infty$ (**3a**): (a) *cis* orientation of one ligand; (b) *trans* orientation of another ligand; (c) their successive occurrence linked by the silver(I) centers.

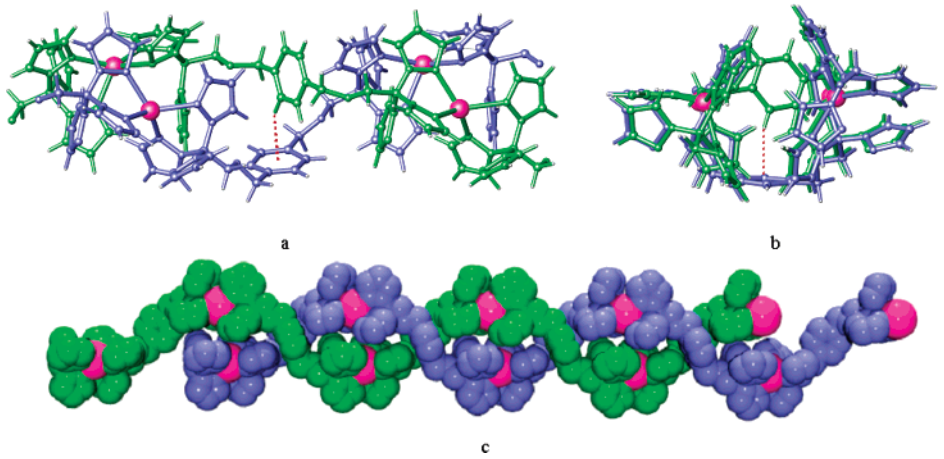

Figure 13. The double stranded helical structure of **3a**: (a) two intertwined strands, view perpendicular to *a* axis, with the C−H···π interaction showed as red dotted lines; (b) the same two strands viewed along the *a* axis; (c) space filling of **3a**.

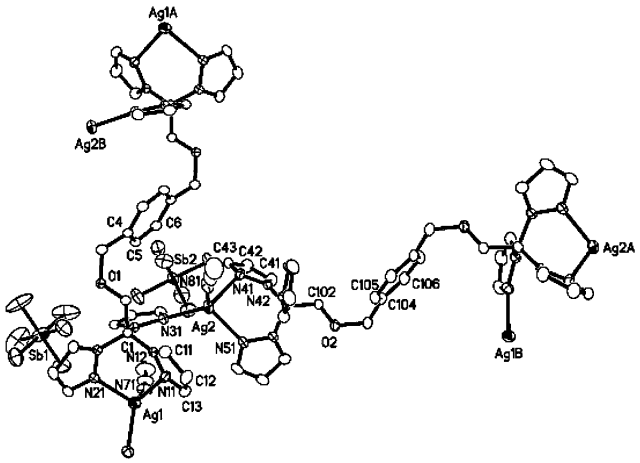

Figure 14. ORTEP representation of the cationic unit in $\{p\text{-}C_6H_4[CH_2OCH_2C(pz)_3]_2[(AgSbF_6)_2(CH_3CN)_2][(CH_3CN)_{0.25}(C_4H_{10}O)_{0.25}]\}_\infty$ (**2b**) with displacement ellipsoids shown at 40% probability level.

hydrogen bonds as observed for the SbF_6^- counterions in the case of **2b**, with all C−H···F distances being greater than the sum of van der Waals radii of hydrogen and fluorine.

Crystallization of **4** from acetonitrile yields crystals of the formula $\{p\text{-}C_6H_4[CH_2OCH_2C(pz)_3]_2[(AgBF_4)_2(CH_3CN)](C_4H_{10}O)\}_\infty$ (**4b**). This compound is a coordination polymer with a sheet structure similar to **2b** and **3b**, organized by a $\kappa^2-\kappa^1$ bonding mode of the tris(pyrazolyl)methane units (Figure 19), but in contrast to the other "type b" structures it contains two types of helical argentachains, one of which does not contain a acetonitrile bonded to the silver(I), Figure 20. The three-coordinate silver in this chain has a flattened trigonal pyramid arrangement (sum of the N−Ag(1)−N bond angles = 347°). In addition, each silver in this chain interacts with the π cloud of a pyrazolyl ring κ^2-coordinated to the next silver(I) atom in the chain.[31] The second type of silver atom has a distorted tetrahedral arrangement with the CH_3CN molecules bonded alternatively above and below the chain. As in other "type b" structures, there are C−H···π interactions supporting the sheet structure. The same pyrazolyl ring that is involved in the silver−π contact acts as a hydrogen donor, with the central arene ring acting as acceptor.

The differences in the coordination environment of silver atoms in **4b** lead to a change in symmetry when compared to **2b** and **3b**. While both **2b** and **3b** crystallize in the triclinic system, space group $P\bar{1}$, **4b** crystallizes in the chiral

(31) (a) Mascal, M.; Kerdelhue, J. L.; Blake, A. J.; Cooke, P. A. *Angew. Chem., Int. Ed.* **1999**, *39*, 1968. (b) Mascal, M.; Kerdelhue, J. L.; Blake, A. J.; Cooke, P. A.; Mortimer, R. J.; Teat, S. J. *Eur. J. Inorg. Chem.* **2000**, 485.

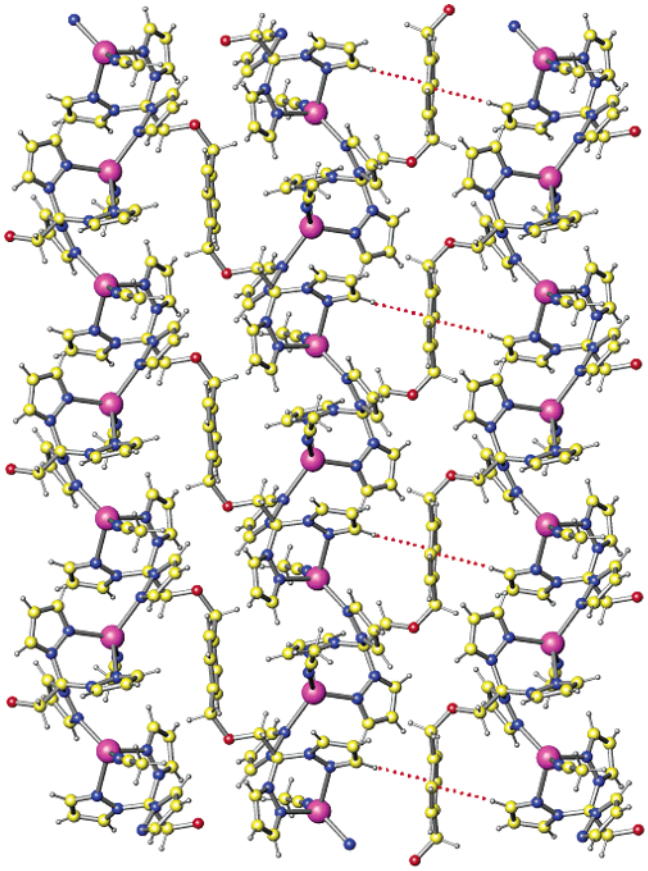

Figure 15. One sheet of **2b**, formed by three argentachains linked by the organic spacers; the red lines represent the C−H···π interactions between two pyrazolyl rings sandwiching one row of central arene rings.

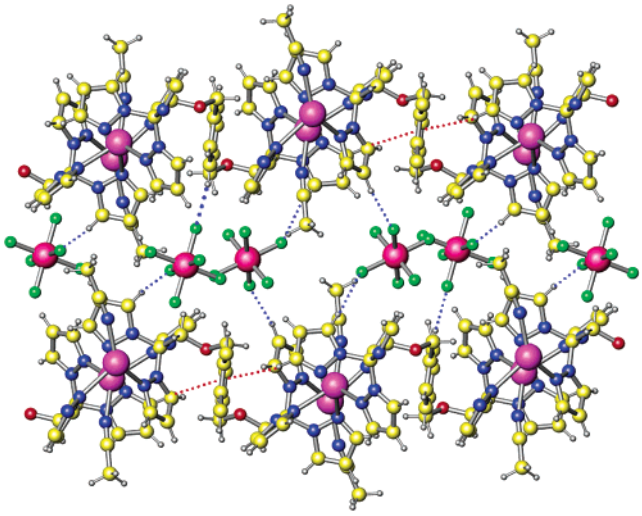

Figure 16. The crystal packing of **2b** showing the C−H···F hydrogen bonds as blue dotted lines; also shown (red dotted lines) are the C−H···π interactions within the sheet structure of **2b**.

orthorhombic space group $P2_12_12_1$. The different coordination environment of silver atoms, coupled with a *trans* orientation of the organic spacer, leads to a helical arrangement of both AgNNCNN argentachains. In both cases, the arrangement of the backbone is helical, but the chirality of each is opposite. Both helices are generated around crystallographic 2_1 screw axes along the *a* axis of the unit cell. For both, the distance between every other silver atom is equal and

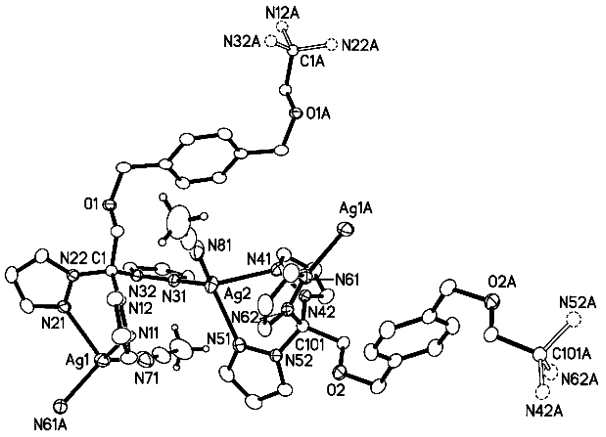

Figure 17. ORTEP representation of the cationic unit in $\{p\text{-}C_6H_4[CH_2OCH_2C(pz)_3]_2[(AgPF_6)_2(CH_3CN)_2][(CH_3CN)_{0.25}(C_4H_{10}O)_{0.25}]\}_\infty$ (**3b**) with displacement ellipsoids shown at 20% probability level.

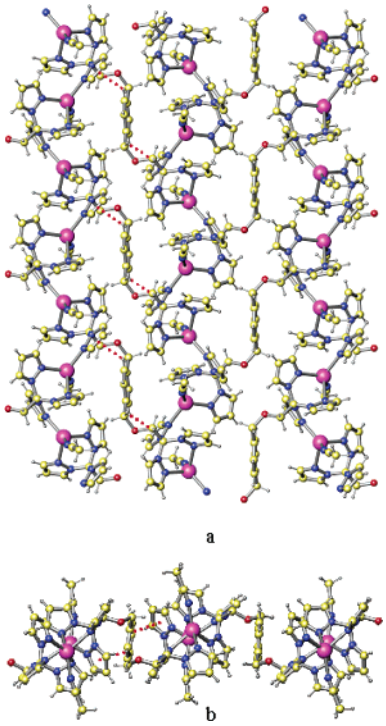

Figure 18. The sheet structure of $\{p\text{-}C_6H_4[CH_2OCH_2C(pz)_3]_2[(AgPF_6)_2(CH_3CN)_2][(CH_3CN)_{0.25}(C_4H_{10}O)_{0.25}]\}_\infty$ (**3b**): (a) view perpendicular to the sheet; (b) an end on view of the same sheet, in both the C−H···π interactions within the sheet are shown as red dotted lines.

identical to the length of the *a* axis of the unit cell, 10.282 Å, making the pitches of both helicates identical.

Figure 21 shows that the 2D network (viewed end on), formed by the helical chains and the connecting organic bridges, is arranged into a 3D supramolecular quaternary structure by C−H···F weak hydrogen bonds. One of the two nonequivalent BF_4^- ions makes four hydrogen bonds with two of the 2D sheets forming the 3D architecture.[24] The second BF_4^- ion makes two hydrogen bonds, one to each of two sheets. A particularly interesting part of the structure is that each diethyl ether molecule is bonded through one terminal methyl group to the BF_4^- counterion that makes four hydrogen bonds and also through the ether oxygen atom to a coordinated acetonitrile.

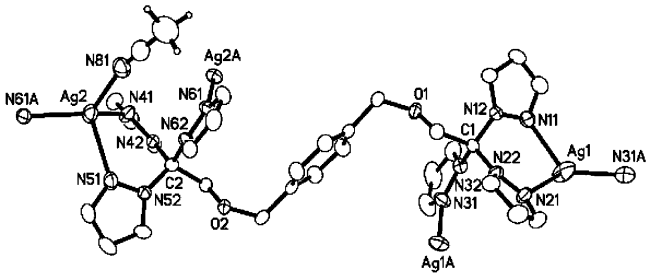

Figure 19. ORTEP representation of the cationic unit of $\{p\text{-}C_6H_4[CH_2OCH_2C(pz)_3]_2[(AgBF_4)_2(CH_3CN)](C_4H_{10}O)\}_\infty$ (**4b**) with displacement ellipsoids shown at 50% probability level.

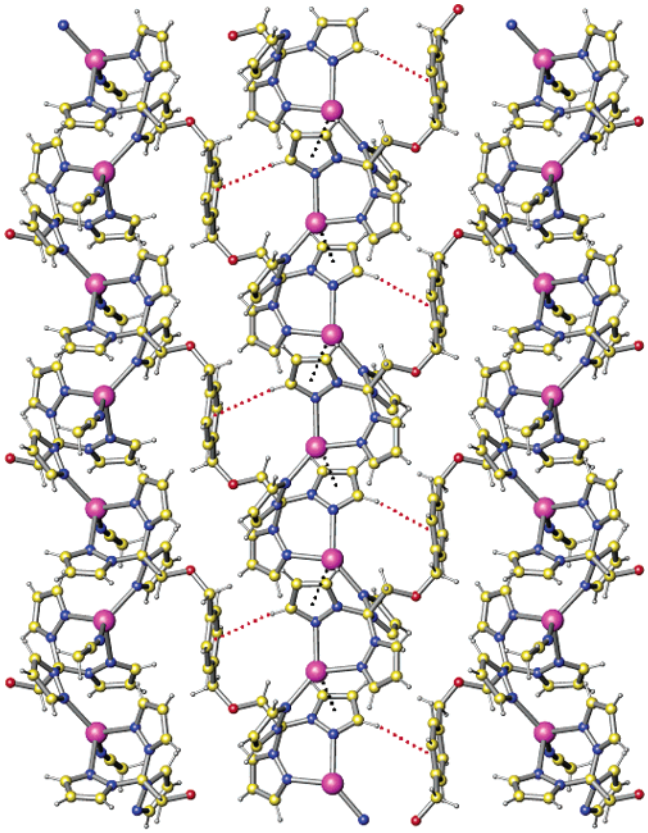

Figure 20. View perpendicular to one sheet formed by the alternating silver chains in **4b**; the C−H···π interactions are shown as red dotted lines and the Ag−π contacts pictured with black dotted lines.

All these interactions build up a chiral network of helices of opposite chirality. This is an example of a racemic mixture of helices crystallizing in a chiral space group, where no symmetry operation relates the two helices of opposite chirality.

Crystallization of **5** from acetonitrile yields crystals of the formula $\{p\text{-}C_6H_4[CH_2OCH_2C(pz)_3]_2(AgNO_3)_2(CH_3CN)_4\}_\infty$ (**5**·4 CH_3CN). The primary structure (Figure 22) is formed again by a $\kappa^2-\kappa^1$ coordination mode of the ligand to the silver(I) centers. In addition, the anions are also coordinated to the silvers, a common feature for discrete silver(I) compounds or silver(I) coordination polymers formed from this counterion.[1c,d,16j,17b] The NO_3^- anion is anisobidentate with one short (2.504(5) Å) and one long (2.761(5) Å) oxygen−silver distance.

The secondary structure again consists of AgNNCNN argentachains, Figure 23. However, the tertiary 2D structure

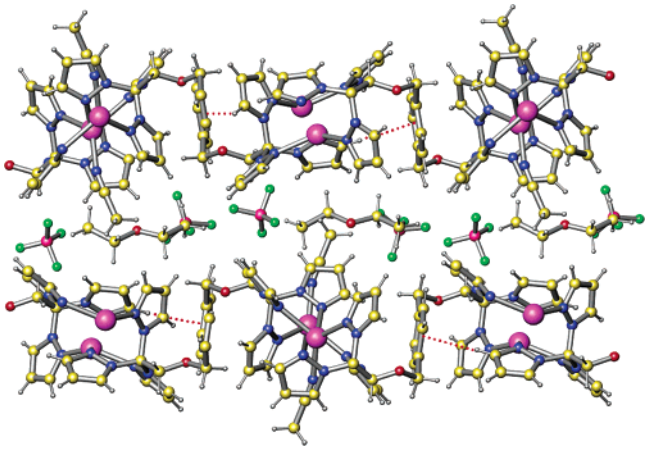

Figure 21. Two sheets in **4b** held together through C−H···F bonds involving the BF_4^- anions, forming a 3-D quaternary architecture; ether molecules situated between the sheets are also shown.

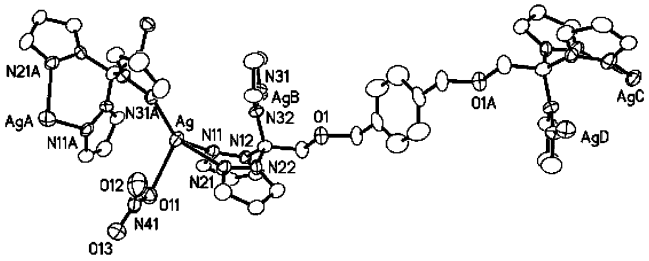

Figure 22. ORTEP representation of $\{p\text{-}C_6H_4[CH_2OCH_2C(pz)_3]_2(AgNO_3)_2\}_\infty$·4$CH_3CN$ (**5**·4CH_3CN), at the 50% probability level with the NO_3^- anions coordinated to silver(I) centers; acetonitrile molecules of solvation and hydrogen atoms not shown.

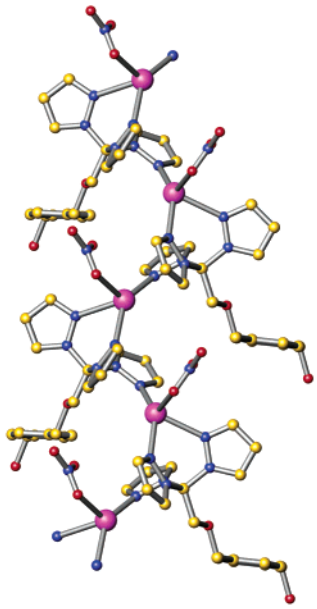

Figure 23. One argentachain of $\{p\text{-}C_6H_4[CH_2OCH_2C(pz)_3]_2(AgNO_3)_2\}_\infty$·4$CH_3CN$ (**5**·4CH_3CN), with the NO_3^- anions coordinated to silver(I) centers; hydrogen atoms not shown.

consists of W-shaped sheets that have an overall configuration very different from **2b**−**4b**. Figure 24 shows two such sheets down the polymeric chains. The sheets are held together in a quaternary structure via a favorable noncovalent interaction that we have named "quadruple pyrazolyl embrace" and presented in detail in Scheme 1: a concerted set

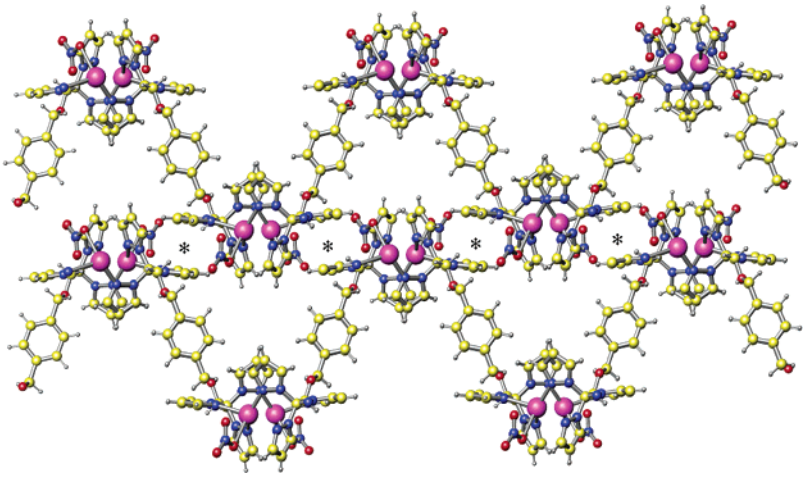

Figure 24. Two stacked sheets of **5**·CH_3CN; the pyrazolyl embrace interactions are centrally pictured and marked with *.

of $\pi-\pi$ stacking and C−H···π interaction.[19] Two closely situated sets of pyrazolyl rings, part of adjacent sheets, within the [C(pz)] units that chelate the silver(I) centers, are involved in this supramolecular contact. Within these four pyrazolyl rings, two of them are stacked and parallel displaced, and they serve as hydrogen donors in the associated C−H···π interaction, where two other pyrazolyl rings act as acceptors. The association between the sheets creates channels that bisect the *b* and *c* axes of the unit cell creating 12 × 10 Å^2 channels that are filled with acetonitrile molecules.

Anion Exchange Properties. The anion exchange properties of these compounds have been explored by treating $\{p\text{-}C_6H_4[CH_2OCH_2C(pz)_3]_2(AgSbF_6)_2\}_\infty$ (**2**) with a saturated aqueous solution of KPF_6 and separately a solution of KO_3SCF_3. The solid was periodically collected by filtration (every 2 h) and the presence of the second anion monitored by infrared spectroscopy following the characteristic bands of the anions.[32,33] Samples containing mixtures of anions as well as ones with the SbF_6^- completely exchanged could be obtained by these methods. The IR spectrum of pure **2** (red line in Figure 25) shows a band at 664 cm^{-1} (marked with *) that is assigned to $\nu_3(T_{1u})$ vibration of the SbF_6^- anion. The IR spectrum of a partially (SbF_6^-/PF_6^-) exchanged sample (after 4 h of stirring) is shown in Figure 25 as a green line; the band at 664 cm^{-1} is still present, but of a weaker intensity, an indication of a decreased quantity of this anion. There are two new bands (both marked with ●) at 841 and 550 cm^{-1}, assigned to $\nu3(T_{1u})$ and $\nu4(T_{1u})$ vibrations of the PF_6^- anion. The anions can be completely exchanged by stirring for 12 h. The IR spectrum of completely (SbF_6^-/PF_6^-) exchanged sample is pictured as a blue line; the band at 664 cm^{-1} is no longer present, and the two strong bands of the PF_6^- anion clearly present. This procedure can be extended to other anions as well: the IR spectrum of a partially ($SbF_6^-/CF_3SO_3^-$) exchanged sample is shown in Figure 25 as a black line. The band at 664 cm^{-1} is still present but again of a weaker intensity, and the band (marked with #) at 1154 cm^{-1} is clearly assigned to $\delta_{as}CF_3(E)$.[27]

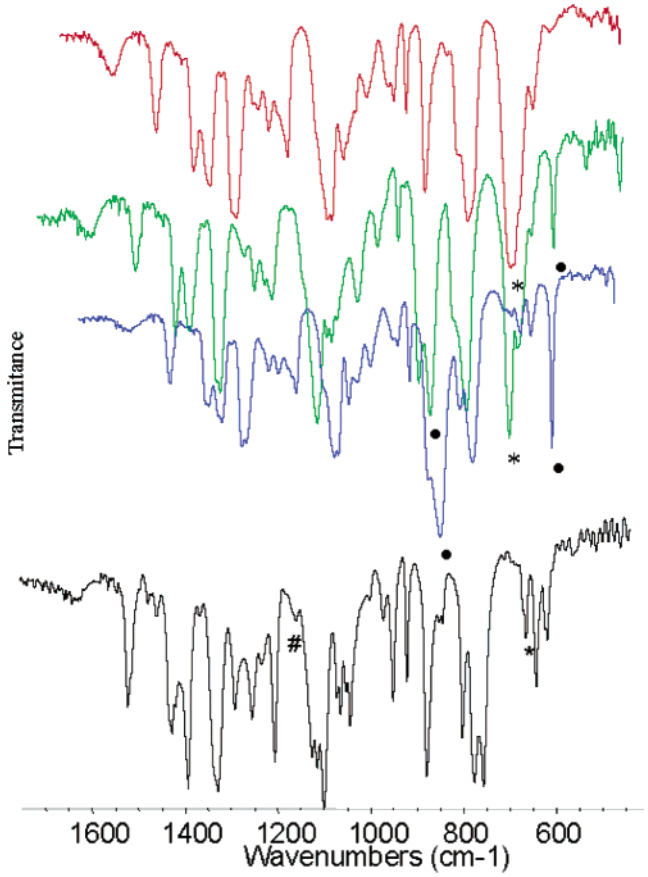

Figure 25. Anion exchange monitored by IR spectroscopy; red line indicates IR spectra of **2**: the band at 664 cm^{-1} (marked with *) is assigned to $\nu_3(T_{1u})$ vibration of the SbF_6^- anion. Green line indicates IR spectra of a partially (SbF_6^-/PF_6^-) exchanged sample: the bands at 841 and 550 cm^{-1} (marked with ●) are assigned to $\nu_3(T_{1u})$ and $\nu_4(T_{1u})$ vibrations of the PF_6^- anion. Blue line indicates IR spectra of a completely (SbF_6^-/PF_6^-) exchanged sample. Black line indicates IR spectra of a partially ($SbF_6^-/F_3CSO_3^-$) exchanged sample: the band at 1154 cm^{-1} (marked with #) is assigned to the $\delta_{as}CF_3(E)$ vibration.

(32) Related examples: (a) Yaghi, O. M.; Li, H. *J. Am. Chem. Soc.* **1996**, *118*, 295. (b) Khlobystov, A. N.; Champness, N. R.; Roberts, C. J.; Tendler, S. J. B.; Thompson, C.; Schroeder, M. *CrystEngComm* **2002**, *4*, 426. (c) Noro, S.; Kitaura, R.; Kondo, M.; Kitagawa, S.; Ishii, T.; Matsuzaka, H.; Yamashita, M. *J. Am. Chem. Soc.* **2002**, *124*, 2568. (d) Sui, B.; Fan, J.; Okamura, T.; Sun, W.-Y.; Ueyama, N. *New J. Chem.* **2001**, *25*, 1379. (e) Jung, O.-S.; Kim, Y. J.; Lee, Y.-A.; Chae, H. K.; Jang, H. G.; Hong, J. *Inorg. Chem.* **2001**, *40*, 2105. (f) Min, K. S.; Suh, M. P. *J. Am. Chem. Soc.* **2000**, *122*, 6834.

(33) Nakamoto, K. *Infrared and Raman Spectra of Inorganic and Coordination Compounds*, 3rd ed.; Wiley-VCH: New York, 1978.

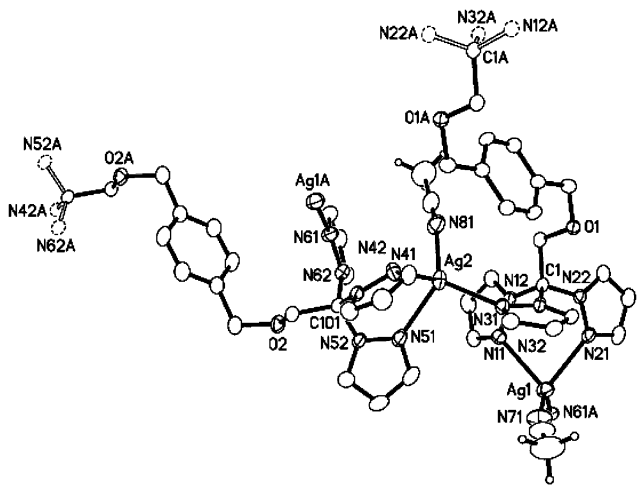

Figure 26. ORTEP representation of the cationic unit of $\{p\text{-}C_6H_4[CH_2OCH_2C(pz)_3]_2[Ag_2(PF_6)_{0.78(1)}(SbF_6)_{1.22(1)}(CH_3CN)_2][(CH_3CN)_{0.25}(C_4H_{10}O)_{0.25}]\}_\infty$ (**6**) with displacement ellipsoids shown at 40% probability level.

From a sample containing a SbF_6^-/PF_6^- mixture of anions, crystals of the formula $\{p\text{-}C_6H_4[CH_2OCH_2C(pz)_3]_2[Ag_2(PF_6)_{0.78(1)}(SbF_6)_{1.22(1)}(CH_3CN)_2][(CH_3CN)_{0.25}(C_4H_{10}O)_{0.25}]\}_\infty$ (**6**) were obtained from the same acetonitrile system used for "b type" complexes and were subjected to X-ray diffraction studies. The cationic unit is shown in Figure 26. A complete structural analysis revealed the same basic 2D sheet structure as observed for **2**−**4b**. Two independent $(P,Sb)F_6^-$ anion positions were located; however, the PF_6^- and SbF_6^- anions were found to be mixed on both sites, in the proportion P(1)/Sb(1) = 0.314(1)/0.686(1) and P(2)/Sb(2) = 0.467(1)/0.543(1). Refinement of either site as fully P or fully Sb resulted in unreasonably small (P) or large (Sb) displacement parameters as well as higher *R*-values. The fluorine atoms in both anion sites are well ordered, and therefore, the P(Sb)−F bond lengths represent a weighted average of the P−F and Sb−F contributions. The slightly inflated displacement parameters for these fluorine atoms may reflect the presence of two closely separated F_6 octahedra, or simply the rotational disorder commonly encountered in spherical anions of this type.

Analysis of the covalently bonded network indicated the presence of two types of C−H···π interactions between the pyrazolyl−central arene ring pairs. Interestingly, both of the interactions in which a pyrazolyl ring acted as the hydrogen donor and the phenyl ring as acceptor as in **2b** and the inverse situation found in **3b** were found, as pictured in Figure 27. In this case, every other row of central arene rings alternatively acts as either hydrogen donor or acceptor. In other words, both interactions found separately in alternate rows in **2b** and **3b** are combined in the case of **6**, in an alternating occurrence, involving every row.

When the SbF_6^- anion was completely exchanged with PF_6^- and a crystalline sample was subjected to crystallographic studies, an identical structure with that of **3b** prepared directly from $AgPF_6$ was obtained.

When the same SbF_6^-/PF_6^- mixture that was used for the growth of the crystals for **6** from acetonitrile was crystallized

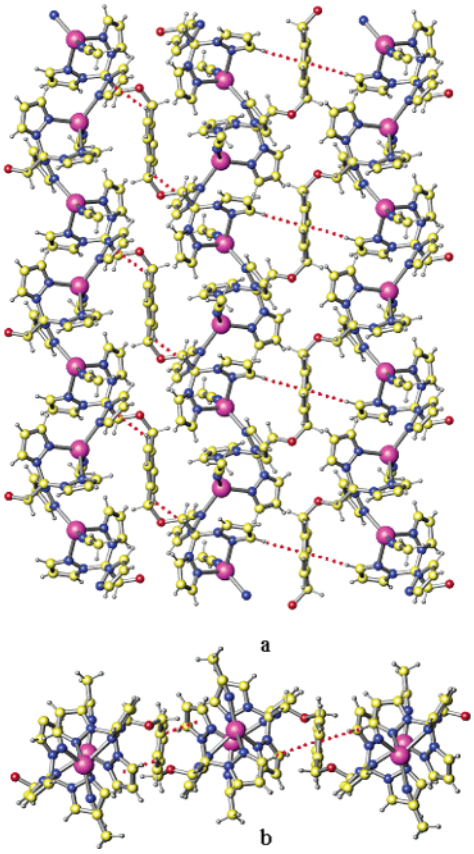

Figure 27. The sheet structure of $\{p\text{-}C_6H_4[CH_2OCH_2C(pz)_3]_2[Ag_2(PF_6)_{0.78(1)}(SbF_6)_{1.22(1)}(CH_3CN)_2][(CH_3CN)_{0.25}(C_4H_{10}O)_{0.25}]\}_\infty$ (**6**); the red dotted lines are the C−H···π interactions.

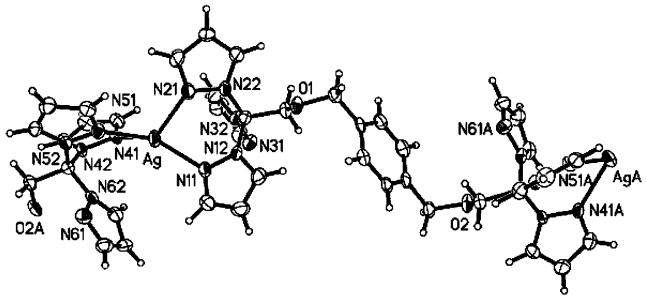

Figure 28. ORTEP representation of the cationic unit of $\{p\text{-}C_6H_4[CH_2OCH_2C(pz)_3]_2(AgSbF_6)[(CH_3)_2CO]_{1.5}\}_\infty$ (**7**) with displacement ellipsoids shown at 50% probability level.

from acetone, a new compound containing only SbF_6^- as the counterion was obtained, of the formula $\{p\text{-}C_6H_4[CH_2OCH_2C(pz)_3]_2(AgSbF_6)[(CH_3)_2CO]_{1.5}\}_\infty$ (**7**). In contrast to its other two SbF_6^- "homologues" **2a** and **2b**, where the tris(pyrazolyl)methane units act in the $\kappa^2-\kappa^1$ coordination mode and the metal-to-ligand ratio is 2:1, here the $[C(pz)_3]$ unit is $\kappa^2-\kappa^0$ bonded with a metal-to-ligand ratio of 1:1 (Figure 28). This feature leads to a 1D secondary structure represented in Figure 29a, where all the ligands have a *trans* arrangement of the sidearms. The tertiary structure is organized by acetone molecules that interact with a pyrazolyl ring via C−H···π interactions, with one of the methyl groups acting as the hydrogen donor, Figure 29b. In addition, the oxygen atoms within the acetones act as acceptors in weak C−H···O hydrogen bonds, where the hydrogen donor is a CH group

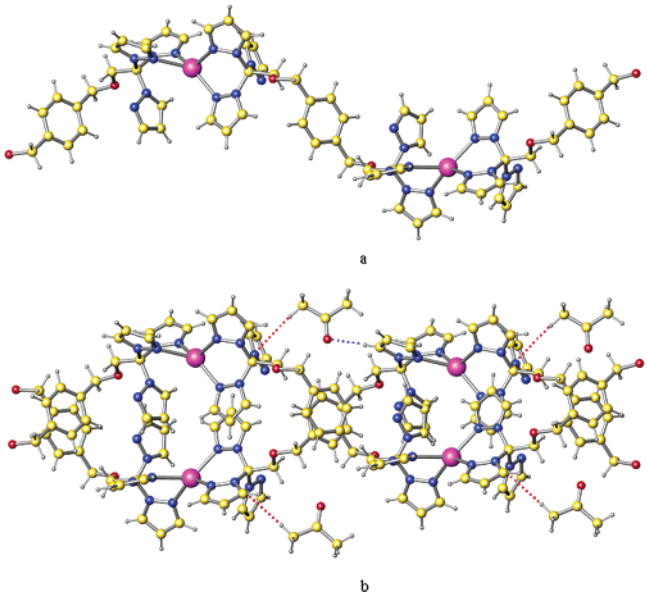

Figure 29. (a) One chain of $\{p\text{-}C_6H_4[CH_2OCH_2C(pz)_3]_2(AgSbF_6)[(CH_3)_2CO]_{1.5}\}_\infty$ (**7**) showing the $\kappa^2-\kappa^0$ bonding mode of the $[C(pz)_3]$ unit and the *trans* arrangement of the ligand; (b) two strands of **7** and their associated acetone molecules (C−H···π contacts showed as red dotted lines). The C−H···O hydrogen bonds responsible for organization of **7** in sheets are shown as a blue dotted line.

from a pyrazolyl ring situated on an adjacent strand. These interactions build up a 2D tertiary structure, arranging the strands closely one to another in a sheetlike structure.

Comparison of "Molecular" and Supramolecular Structures. The structural behavior of the silver(I)−p-$C_6H_4[CH_2OCH_2C(pz)_3]_2$ system with noncoordinating counterions shows a dual solvent−counterion dependence. The solvent used for crystallization primarily controls the structures. When the compounds are crystallized from the coordinating solvent acetonitrile, similar 2-D sheet structures are observed ("b type"), with the anions imposing small differences within the sheets. When crystallized from the weakly coordinating solvent acetone ("a type"), the anions impose major structural variations of the resulting architectures.

In all "a type" structures, helical arrangements were observed, either of the argentachains (**1a**), of the organic spacer only (**2a**), or of the whole 1-D covalent network (**3a**). Given the major differences in the secondary structures of **1a** and **2a**, there are surprising similarities: both compounds crystallize in the rhombohedral space group $R\bar{3}$ (hexagonal setting), both with $Z = 9$. In both compounds, the $\kappa^2-\kappa^1$ coordination mode of the ligand is present, and both tertiary structures are supported by the same double $\pi-\pi$ stacking where two pyrazolyl rings (symmetry related) sandwich the central arene core. In both compounds the local structure of the ligand is almost identical: the ether-based sidearms have a skewed *trans* arrangement with the angle formed by the arene ring and the plane of the attached CH_2OCH_2 group being around 42°. This orientation of the ligand is required by the double $\pi-\pi$ stacking in which the ligand is involved.

In the case of **1a**, the F···F interactions, coupled with the extensive network of weak hydrogen bonds between the triflate oxygen atoms and C−H groups on the ligands, organize the tubular tertiary structure of helical argentachains. The double $\pi-\pi$ stacking interactions in the organic linkers are critical to the circular organization of these argentachains (Figures 2 and 3). In the case of **2a**, the acetone molecules noncovalently connected to the covalent framework along with the "trapped" SbF_6^- counterion appear to support the tubular organization of the argentamacrocycles with the helical organization of the L−Ag−L−Ag sequence also important to this arrangement.

Among the helical systems, DNA is certainly the most commonly known example. The DNA double helix is formed upon self-assembly of two complementary helical strands. The driving force for the formation of the double helical arrangement is the establishment of hydrogen bonds between complementary nucleic acid bases. However, in principle, any type of attractive interaction may be used to generate double helical architectures, as long as there are two complementary helical strands with complementary recognition sites that will induce a recognition pattern within their structure. In the case of **3a**, the self-complementary recognition pattern is played by the central arene ring that undergoes a C−H···π interaction, as pictured in Figure 13.

The crystalline solids obtained from acetonitrile, "b type", show similar structures; two-dimensional sheets build up by linking the AgNNCNN sequence of argentachains by the organic spacer. Although the covalent part of the **2b**−**4b** networks is two-dimensional, the structures have thickness. The views of **2b** (Figure 16), **3b** (Figure 18b), and **4b** (Figure 21) in the same alignment of the sheets illustrate the similarity in the width of the sheets. Also shown are U-shaped channels formed between the silver strands by the 1,4-bis[ethoxymethyl]benzene bridge. The dimensions of the channels are ca. 6 × 4 Å^2 in all structures, as measured between the two methylene groups directly bonded to the phenyl ring and between these methylene groups and the central methine carbon atoms from the tris(pyrazolyl)methane units. Despite the similarity between the sheets, subtle differences induced by the anions are also present (vide supra). The differences between **2b** and **3b** are at the noncovalent level only, but when **4b** is compared with its analogues a drastic change in symmetry is observed. The asymmetric units of **2b** and **3b** contain two crystallographically inequivalent Ag atoms and two independent anions; two ligands are situated about crystallographic inversion centers, and therefore, only half of each ligand is present. The asymmetric unit of **4b** is composed also of two crystallographically inequivalent Ag atoms and two independent anions, but one full ligand is present. Further, the coordinated acetonitrile molecules are bonded to only one type of silver. These differences lead to the following situation: in the case of **2b** and **3b** the inequivalent Ag atoms are found alternatively in the same argentachain, while in the case of **4b** the inequivalent Ag atoms are found in different chains. An additional important structural difference is that in **4b** the solvent molecules are held between the helical layers in a very ordered fashion by weak hydrogen bonds, a rather unusual observation for helical superstructures.[1a] In **2b** and **3b** (where the solvent is not involved in any

noncovalent interaction) the trapped solvent was found to be disordered.

When the structure of **5**·4 CH_3CN, containing the coordinating counterion nitrate, is compared with its homologues, the differences are even more pronounced. The nitrates coordinate to the silvers, and the acetonitrile molecules in the crystals are simply solvents of crystallization. This alteration imposes a change in the structure from an almost planar sheet to a W-shaped sheet (compare Figures 16, 18b, 21, and 27b with Figure 24). Also different is the packing of the sheets within the crystal that is controlled by the pyrazolyl embrace in **5**·4CH_3CN.

Crystallization of the partially exchanged SbF_6^-/PF_6^- mixture from both acetonitrile and acetone leads to two very different complexes. From acetonitrile, a "b type" structure of the mixed counterion species **6** is observed. In the presence of both anions, both types of C−H···π interactions are observed that are found separately in **2b** and **3b** (see Figures 15, 16, 18, and 27).

Crystallization of the SbF_6^-/PF_6^- mixture from acetone produces a complex with the formula $\{p\text{-}C_6H_4[CH_2OCH_2C(pz)_3]_2(AgSbF_6)[(CH_3)_2CO]_{1.5}\}_\infty$ (**7**), containing only the SbF_6^- anion and with different stoichiometry than its two SbF_6^- "homologues" **2a** and **2b**. The presence of the PF_6^- in the crystallization solution leads to precipitation of a new SbF_6^- complex that is very different from the **2a** and **2b** complexes. As observed with **2a**, acetone molecules are involved in organizing the association of the coordination polymer into a higher level of organization (see Figure 29). As expected from the similar stoichiometry, the $\kappa^2-\kappa^0$ behavior of the $[C(pz)_3]$ unit in **7** (Figure 29a) is the same as in **3a** (Figures 11, 12), but the ligand has only the *trans* orientation. The missing *cis* orientation of the ligand impedes the formation of the single and the subsequent double stranded helical organization as in the case of **3a**. Interestingly, the alignment of the strands with the central arene cores situated close one to another shows the incipient formation of weak C−H···π interactions somewhat analogous to those observed with **3a**.

The formation process for **7** is unique in this work. Using biological systems, Lindsey[34] has identified several types of self-assembly processes, and besides the "strict" self-assembly process, we mention here only a few: (a) irreversible self-assembly (irreversible reactions kinetically channeled to a particular pathway); (b) assisted self-assembly (where an external species prevents the formation of unwanted intermediates and does not appear in the final product); (c) directed self-assembly (where a species directs the course of the assembly but is not present in the final product). While all the processes leading to the self-assembly of **1**−**6** (either type a or b) are the "strict" self-assembly process, the assembly of **7** is a "directed" self-assembly process. The presence of the PF_6^- anion in solution "influences" a $\kappa^2-\kappa^0$ coordination mode of the $[C(pz)_3]$ unit as observed in the "pure" PF_6^- sample, when both are crystallized from acetone. Although in the case of **3a** and **7** the bulk starting material in the crystallization process was a compound with a ligand-to-metal ratio of 1:2, both the final crystalline compounds were found to have a ligand-to-metal ratio of 1:1, a phenomenon found only in the case where PF_6^- was the counterion and acetone was used as crystallization solvent.

(34) Lindsey, J. S. *New J. Chem.* **1991**, *15*, 153.

Conclusion

Critical for the formation of these supramolecular structures is the organization inherently built into the bitopic ligand by its rigid parts (central arene core and $[C(pz)_3]$ units) linked by a set of three sp^3 hybridized atoms. Importantly, it is the flexibility of the ether linkage that allows the anions to organize the structures reported here; rigid ligands would have to be perfectly tailored to allow such structures, and their inherent rigidity would restrict the influence of the anions in the final structures.

Summing all the findings for this system, we observed that all counterions impose changes in the overall structures of the crystalline solids, but those differences are much greater when the material is crystallized from a noncoordinating solvent. The following essential patterns in the self-assembly processes were found in these structures: (a) the ligand displays a $\kappa^2-\kappa^1$ coordination mode of the $[C(pz)_3]$ units in all cases, except the cases when the PF_6^- anion was present and the crystallization solvent was acetone (**3a** and **7**) where the coordination mode was $\kappa^2-\kappa^0$; (b) the ligand was able to adjust its structure to maximize both covalent and noncovalent interactions; (c) there are the absence of coordinated acetone molecules in "a type" structures and the presence of coordinated acetonitrile molecules in "b type" structures; (d) there are the involvement of OTf^-, SbF_6^-, and BF_4^- anions in weak C−H···O(F) hydrogen bonds and the lack of such interactions in the PF_6^- case; (e) the coordination of NO_3^- to silver(I) center contrasts to that of OTf^- anion that is also known to be sometimes a coordinating anion.

An important result of these patterns is the demonstration, particularly with **1a** and **2a**, of success using a noncovalent strategy for the assembly of covalent networks with remarkable topologies. Although the three-dimensional structures of both of these compounds are built on covalent bonds, the tertiary structures observed appear to be arranged by the noncovalent bonds. This contention is strongest for **1a** where the $[(CF_3SO_3)_6]^{6-}$ clusters are held together by weak F···F interactions and then these clusters organize the covalent structure through weak C−H···O hydrogen bonds with the bitopic ligand involving the $-SO_3$ groups. For **2a**, the six acetone molecules and one SbF_6^- anion present between the argentamacrocycles also organize the tubular structure observed. For **3a**, the covalent bonds organize the strands, but weak C−H···π interactions between the central arene rings organize the double helix. Crystallization of these systems from weakly coordinating solvents is necessary to allow these weak forces to dominate the structures: the three-coordinate silver centers appear to be more flexible in accommodating particular structures than the four-coordinate silvers in the complexes crystallized from acetonitrile. In

these cases, the coordination of the solvent influences the system such that sheet structures are observed in all cases.

NMR and ES/MS studies show that in solution the cationic species present are anion independent and that in solutions of coordinating solvents a complicated series of equilibria take place between ligand−silver(I) species, species in which the solvent has partially or completely displaced the ligands. The structural diversity observed in the solid state, triggered by the anion and/or solvent, must develop in the final crystallization step.

The structures reported here demonstrate that the bitopic *p*-$C_6H_4[CH_2OCH_2C(pz)_3]_2$ ligand is structurally adaptive; that is, it can adjust its structure to maximize all covalent and noncovalent forces within a given system. With this ability to adjust to changes in the system, coupled with the ability to participate in $\pi-\pi$ stacking and form C−H$\cdots\pi$ and weak hydrogen bonding interactions, the $C_6H_{6-n}[CH_2OCH_2C(pz)_3]_n$ class of ligands based on linking tris(pyrazolyl)methane units with semirigid organic spacers contains ideal candidates for studying the self-assembly process. We have also shown that although the structures reported here are very different, several important similarities can be found. This strategy for the assembly of covalent networks based on semirigid ligands completes the gap between strategies based on rigid or completely flexible ligands.

Experimental Section

General Procedure. All operations were carried out under a nitrogen atmosphere using standard Schlenk techniques and a Vacuum Atmospheres HE-493 drybox. All solvents were dried and distilled prior to use following standard techniques. The ^{1}H NMR spectra were recorded on a Varian AM300 spectrometer using a broad-band probe. Proton chemical shifts are reported in ppm versus internal Me_4Si. IR spectra were recorded on a Nicolet 5DXBO FTIR spectrometer. Electrospray ionization mass spectrometry data were obtained on a MicroMass QTOF spectrometer. Clusters assigned to specific ions show appropriate isotopic patterns as calculated for the atoms present. Elemental analyses were performed by Robertson Microlit Laboratories (Madison, NJ). Tris-2,2,2-(1-pyrazolyl)ethanol, $HOCH_2C(pz)_3$, and *p*-$C_6H_4[CH_2OCH_2C(pz)_3]_2$ (**L**) were prepared following literature methods.[18a]

Synthesis of {*p*-$C_6H_4[CH_2OCH_2C(pz)_3]_2(AgO_3SCF_3)_2$}$_\infty$ (1). A THF (20 mL) solution of *p*-$C_6H_4[CH_2OCH_2C(pz)_3]_2$, **L**, (0.295 g, 0.500 mmol) was added dropwise to a solution of AgO_3SCF_3 (0.256 g, 1.00 mmol) in dry THF (20 mL) under an inert atmosphere. A white precipitate appeared as the mixture was stirred for 2 h. The THF was removed by cannula filtration and the white precipitate washed with THF (2 × 10 mL) and then vacuum-dried to afford 0.413 g (75%) of solid identified as {*p*-$C_6H_2[CH_2OCH_2C(pz)_3]_4(AgO_3SCF_3)_2$}$_\infty$. ^{1}H NMR (acetone-$d_6$): δ 7.84, 7.81, (d, d, J = 1.9, 2.7 Hz, 6,6H, 3,5-H *pz*), 7.10 (s, 4H, C_6H_4), 6.59 (dd, 6H, J = 1.9, J = 2.7 Hz, 4-H *pz*), 5.03 (s, 4H, OCH_2Ph), 4.68 (s, 4H, OCH_2C(pz)$_3$). Calcd for $C_{32}H_{30}Ag_2F_6N_{12}O_8S_2$: C, 34.80; H, 2.74; N, 15.22. Found: C, 34.97; H, 2.69, N, 15.30. ES$^+$/MS: 699 and 955 corresponding to $[LAg]^+$ and $[LAg_2O_3SCF_3]^+$.

Synthesis of {*p*-$C_6H_4[CH_2OCH_2C(pz)_3]_2(AgSbF_6)_2$}$_\infty$ (2). This compound was synthesized as above for **1** using $AgSbF_6$ (0.343 g, 1.00 mmol), to afford 0.510 g (79%) of solid identified as {*p*-$C_6H_2[CH_2OCH_2C(pz)_3]_4(AgSbF_6)_2$}$_\infty$. ^{1}H NMR (acetone-$d_6$): δ 7.82, 7.77 (m, m, 6,6H, 3,5-H *pz*), 7.09 (s, 4H, C_6H_4), 6.57 (m, 6H, 4-H *pz*), 5.02 (s, 4H, OCH_2C(pz)$_3$), 4.67 (s, 4H, OCH_2Ph). Calcd for $C_{30}H_{30}Ag_2F_{12}N_{12}O_2Sb_2$: C, 28.20; H, 2.37; N, 13.15. Found: C, 28.51; H, 2.21; N, 13.17. ES$^+$/MS: *m*/*z* 699 and 1041, corresponding to $[LAg]^+$ and $[LAg_2SbF_6]^+$.

Synthesis of {*p*-$C_6H_4[CH_2OCH_2C(pz)_3]_2(AgPF_6)_2$}$_\infty$ (3). This compound was synthesized as above for **1** using $AgPF_6$ (0.254 g, 1.00 mmol), to afford 0.409 g (74%) of solid identified as {*p*-$C_6H_2[CH_2OCH_2C(pz)_3]_4(AgPF_6)_2$}$_\infty$. ^{1}H NMR (acetone-$d_6$): δ 7.83, 7.76 (m, m, 6,6H, 3,5-H *pz*), 7.08 (s, 4H, C_6H_4), 6.59 (m, 6H, 4-H *pz*), 5.01 (s, 4H, OCH_2C(pz)$_3$), 4.65 (s, 4H, OCH_2Ph). Calcd for $C_{30}H_{30}Ag_2F_{12}N_{12}O_2P_2$: C, 32.87; H, 2.76; N, 15.33. Found: C, 33.05; H, 3.15; N, 14.99. ES$^+$/MS: *m*/*z* 699 corresponding to $[LAg]^+$.

Synthesis of {*p*-$C_6H_4[CH_2OCH_2C(pz)_3]_2(AgBF_4)_2$}$_\infty$ (4). This compound was synthesized as above for **1** using $AgBF_4$ (0.195 g, 1.00 mmol), to afford 0.445 g (84%) of solid identified as {*p*-$C_6H_4[CH_2OCH_2C(pz)_3]_2Ag_2(BF_4)_2(THF)$}$_\infty$. ^{1}H NMR (acetone-$d_6$): δ 7.82, 7.77 (m, m, 6,6H, 3,5-H *pz*), 7.09 (s, 4H, C_6H_4), 6.57 (m 6H, 4-H *pz*), 5.02 (s, 2H, OCH_2Ph), 4.67 (s, 2H, OCH_2C(pz)$_3$), 3.62 (m, 2H, CH_2O THF), 1.92 (m, 2H, CH_2 THF). Calcd for $C_{30}H_{30}Ag_2B_2F_8N_{12}O_2\cdot C_4H_8O$: C, 38.81; H, 3.64; N, 15.98. Found C, 38.86; H, 3.55; N, 16.23. ES$^+$/MS: *m*/*z* 699 and 893, corresponding to $[LAg]^+$ and $[LAg_2BF_4]^+$.

Synthesis of {*p*-$C_6H_4[CH_2OCH_2C(pz)_3]_2(AgNO_3)_2$}$_\infty$ (5). This compound was synthesized as above for **1** using $AgNO_3$ (0.167 g, 1.00 mmol) in dry acetonitrile (15 mL) under an inert atmosphere. The clear solution was stirred for 2 h, and 100 mL of diethyl ether was added, resulting in the precipitation of a white compound. The solvents were removed by cannula filtration and the white precipitate washed with THF (2 × 10 mL) and then vacuum-dried to afford 0.306 g (66%) of solid identified as {*p*-$C_6H_2[CH_2OCH_2C(pz)_3]_4(AgNO_3)_2$}$_\infty$. ^{1}H NMR (acetone-$d_6$): δ 7.82, 7.77 (m, m, 6,6H, 3,5-H *pz*), 7.09 (s, 4H, C_6H_4), 6.57 (m 6H, 4-H *pz*), 5.02 (s, 4H, OCH_2Ph), 4.67 (s, 4H, OCH_2C(pz)$_3$). Calcd for $C_{30}H_{30}Ag_2N_{14}O_8$: C, 38.73; H, 3.25; N, 21.08. Found: C, 38.52; H, 3.02; N, 20.88. ES$^+$/MS: *m*/*z* 699 and 868, corresponding to $[LAg]^+$ and $[LAg_2NO_3]^+$.

Crystallization Procedure. In a typical crystallization procedure, a sample of about 5 mg was dissolved in ca. 3 mL of solvent (acetone or acetonitrile). To remove any potential insoluble materials, this solution was filtered through cotton into a small test tube via a pipet. The open small test tube was inserted in a second, larger one that already had ca. 20 mL of diethyl ether and was closed with a Teflon screw cap. The test tubes were kept at room temperature for several days, during which time colorless crystals suitable for X-ray diffraction studies formed.

Anion Exchange Procedure. A 100 mg sample of **2** was suspended in a saturated aqueous solution of KPF_6 or KO_3SCF_3 (50 mL), stirred, filtered, washed with water (100 mL), and air-dried. The anion exchange was monitored by IR spectroscopy (KBr pellets). The first notable anion exchange was observed after the sample was stirred for 0.5 h. The sample used in the crystallization of **6** and **7** was obtained after 4 h of stirring. After 12 h of stirring, the anion was completely exchanged.

Crystallography. All crystals were mounted on thin glass fibers with inert oil or epoxy. After preliminary crystal quality, symmetry and unit cell parameter determination, a full sphere (**1a**, **2b**, **3b** and **6**), approximately $^3/_4$ of a sphere (**3a**), or a hemisphere (**2a**, **4b**, **5b**) of X-ray intensity data was collected at the temperatures indicated in tables in the Supporting Information on a Bruker SMART APEX CCD-based diffractometer (Mo Kα radiation, λ = 0.71073 Å).[35] Raw area detector data frame integration and Lorentz/polarization corrections were carried out with SAINT+.[35] Final unit

cell parameters are based on the least-squares refinement of all reflections with $I > 5\sigma(I)$ from each data set. For **1a**, **2a**, **2b**, **3b**, **4b**, **6**, and **7**, an empirical absorption correction based on the multiple measurement of equivalent reflections was applied with SADABS.[35] Direct methods structure solution (except where noted), difference Fourier calculations, and full-matrix least-squares refinement against F^2 were performed with SHELXTL for all structures.[36]

Compound **1a** crystallizes in the space group $R\bar{3}$ (hexagonal setting) with $Z = 9$ for the given formula. The space group choice was confirmed by the successful solution and refinement of the data; higher symmetry space groups were ruled out on the basis of systematic absences in the intensity data and by manual examination of the completed structure, supported by the ADDSYM routine in PLATON.[37] All atoms are on positions of general crystallographic symmetry. The central phenyl ring of the ligand is situated about an inversion center at 0, $^1/_2$, 0. The asymmetric unit consists of the Ag atom, half a ligand, and the triflate anion. Non-hydrogen atoms were refined with anisotropic displacement parameters; hydrogen atoms were placed in geometrically idealized positions and included as riding atoms.

Compound **2a** also crystallizes in the space group $R\bar{3}$ (hexagonal setting). This space group was confirmed in the same manner as for **1a**. The asymmetric unit contains one Ag atom, half a ligand, an acetone molecule of crystallization, and two crystallographically independent SbF_6^- counterions. Significant positional and occupational disorder was encountered for both SbF_6^- counterions. Sb1 was modeled as occupying a split position, Sb1A and Sb1B, with six surrounding F atoms. Sb2, located on the origin, was modeled with eight surrounding F atoms having suitable occupancies. The central Sb of both SbF_6^- anions exhibited unusually large displacement parameters when refined as fully occupied, notwithstanding the F atom disorder. In addition, full occupancy of both SbF_6^- positions would violate charge balance. Refinement of the site occupation factors (sof's) for each Sb led to a large drop in *R*-values (from ca. 20% at that stage of refinement) and resulted in ellipsoids of a reasonable magnitude. Refinement of the sof's led to values appropriate to maintain electroneutrality within the crystal; subsequently, the sof's were fixed at those values. Eventually all non-hydrogen atoms were refined with anisotropic displacement parameters; hydrogen atoms were idealized and included as riding atoms. The largest residual electron density peaks (ca 1.35 $e^-/Å^3$) are located in the vicinity of the disordered SbF_6^- anions.

In the case of **3a**, systematic absences in the intensity data were consistent with the space groups $P2_1$ or $P2_1/m$; intensity statistics indicated $P2_1$. After initial failure to achieve a reasonable solution in $P2_1/m$, a successful solution and refinement was achieved in $P2_1$. Subsequently, the absence of mirror symmetry was confirmed by manual examination of the structure, as well as by ADDSYM/PLATON.[37] To eliminate the possibility that the significant ligand and anion disorder present in the final refined structure generated erroneously low symmetry, ADDSYM was also performed on a partial structural model including only the atomic positions of the Ag and P atoms, yielding the same results. Application of Patterson methods in the space group $P2_1$ initially located the positions of two Ag atoms and the two P atoms of the PF_6^- anions. Subsequent difference Fourier syntheses revealed the rest of the non-hydrogen atoms in the structure. The asymmetric unit contains two independent sets each of Ag atoms, organic ligands, and PF_6^- anions. The refinement was hampered by major disorder affecting the $-CH_2OCH_2C(pz)_3$ tripodal end of one of the two independent ligands. An arduous effort to model the disorder of the pyrazolyl rings in this region of the structure as three superimposed $\kappa^2-\kappa^0$ orientations was unsuccessful; therefore, only the major disorder component was included. Due to the severity of the disorder, these pyrazolyl rings were fit to regular pentagons whose size was allowed to vary (SHELX AFIX 59 command) and refined with isotropic displacement parameters. A total of 33 restraints was employed. Disorder was also observed in one of the two PF_6^- anions. This anion was modeled as eight $^3/_4$-occupied F atoms surrounding the central P. With the exception of the ligand atoms affected by disorder, all non-hydrogen atoms were eventually refined with anisotropic displacement parameters. Hydrogen atoms were idealized and included as riding atoms. The final refined value of the absolute structure (Flack) parameter is 0.04(3), indicating the correct absolute structure and the absence of racemic twinning.

Compounds **2b** and **3b** crystallize in the triclinic system. The space group $P\bar{1}$ was assumed and confirmed in each case by the successful solution and refinement of the structure. The asymmetric units contain two crystallographically inequivalent Ag atoms and two independent SbF_6^- anions. Two ligands are situated about crystallographic inversion centers, and therefore, only half of each ligand is present in the asymmetric units. A region of disordered solvent is also present in the crystals, which was modeled as 1/4 Et_2O and 1/4 CH_3CN, both disordered about an inversion center. Eventually, all non-H and nonsolvent atoms were refined with anisotropic displacement parameters; the solvent molecules were refined isotropically. A total of 7 geometric restraints were used in modeling the solvent disorder (SHELX SAME and DFIX). Hydrogen atoms were idealized and included as riding atoms.

For **4b** the pattern of systematic absences in the intensity data uniquely determined the orthorhombic space group $P2_12_12_1$. All non-hydrogen atoms were refined with anisotropic displacement parameters; hydrogen atoms were idealized and included as riding atoms.

Though metrically consistent with the orthorhombic crystal system, the pattern of systematic absences in the intensity data of **5b** was not consistent with any orthorhombic space group. Processing the data in the monoclinic system (with $\beta = 90.000(4)°$) gave absences uniquely consistent with the monoclinic space group $P2_1/c$. The structure was readily solved in $P2_1/c$. After location of all heavy atoms, the refinement "hung up" at R1 $\sim$ 25%. Refinement of the data including a correction for pseudo-orthorhombic twinning resulted in a reduction of R1 from $\sim$25% to 6.2% and gave reasonable atomic displacement parameters and residual electron density ($+2.47/-1.68$ $e^-/Å^3$, near Ag). The twin law is $(100/0\bar{1}0/00\bar{1})$, corresponding to a 2-fold rotation around the *a* axis. Such twinning is relatively common in monoclinic crystals with β coincidentally near 90°.[36] Upon successful solution and twin refinement in $P2_1/c$, a check for missed symmetry was performed with the ADDSYM routine in PLATON,[37] which verified the crystal system and space group choice.

The asymmetric unit of **5b** contains one Ag ion, half a ligand situated about an inversion center, one nitrate counterion, and two acetonitrile molecules of crystallization. All atoms reside on positions of general crystallographic symmetry. Non-hydrogen atoms were refined with anisotropic displacement parameters. Hydrogen atoms were idealized and included as riding atoms.

Compound **6** crystallizes in the triclinic system. The space group $P\bar{1}$ was assumed and confirmed by successful solution and

(35) *SMART Version 5.625, SAINT+ Version 6.22 and SADABS Version 2.05*; Bruker Analytical X-ray Systems, Inc.: Madison, WI, 2001.
(36) Sheldrick, G. M. *SHELXTL Version 6.1*; Bruker Analytical X-ray Systems, Inc.: Madison, WI, 2000.
(37) PLATON: (a) Spek, A. L. *Acta Crystallogr., Sect. A* **1990**, *46*, C34. (b) Spek, A. L. *PLATON, A Multipurpose Crystallographic Tool*; Utrecht University: Utrecht, The Netherlands, 2002.

Table 1. Selected Crystal and Structure Refinement Data

	1a	2a	3a	2b	3b	4b	5·4 CH_3CN	6	7
formula	$C_{32}H_{30}Ag_2F_6N_{12}O_8S_2$	$C_{36}H_{42}Ag_2F_{12}N_{12}O_4Sb_2$	$C_{30}H_{30}AgF_6N_{12}O_2P$	$C_{35.50}H_{39.25}Ag_2F_{12}N_{14.25}O_{2.25}Sb_2$	$C_{35.50}H_{39.25}Ag_2F_{12}N_{14.25}O_{2.25}P_2$	$C_{36}H_{43}Ag_2B_2F_8N_{13}O_3$	$C_{38}H_{42}Ag_2N_{18}O_8$	$C_{35.50}H_{39.25}Ag_2F_{12}N_{14.25}O_{2.25}P_{0.78}Sb_{1.22}$	$C_{34.50}H_{39}AgF_6N_{12}O_{3.50}Sb$
fw, g mol^{-1}	1104.54	1394.06	843.50	1388.80	1207.24	1095.19	1094.64	1317.99	1021.40
cryst syst	trigonal	trigonal	monoclinic	triclinic	triclinic	orthorhombic	monoclinic	triclinic	monoclinic
space group	$R\bar{3}$	$R\bar{3}$	$P2_1$	$P\bar{1}$	$P\bar{1}$	$P2_12_12_1$	$P2_1/c$	$P\bar{1}$	$P2_1/c$
a, Å	29.9011(10)	31.3014(18)	15.3714(14)	10.4341(6)	10.3981(8)	10.2820(7)	12.131(2)	10.4348(11)	14.8013(12)
b, Å	29.9011(10)	31.3014(18)	13.5220(12)	15.4008(9)	15.1727(11)	20.2872(14)	19.079(4)	10.4348(11)	30.058(2)
c, Å	11.7415(6)	12.7921(11)	18.0243(16)	15.8447(9)	15.9055(12)	20.5518(14)	9.6355(19)	15.8339(16)	8.7987(7)
α, deg	90	90	90	77.7240(10)	79.326(2)	90	90	78.255(2)	90
β, deg	90	90	114.519(2)	77.4120(10)	77.1400(10)	90	90.000(4)	77.464(2)	92.368(2)
γ, deg	120	120	90	78.3260(10)	78.0300(10)	90	90	78.424(2)	90
Z	9	9	4	2	2	4	2	2	4
R1[a]	0.0372	0.0591	0.0694	0.0339	0.0452	0.0388	0.0624	0.0389	0.0650
wR2[b]	0.0678	0.1794	0.1751	0.0771	0.1146	0.0913	0.1452	0.0943	0.1860

[a] $R1 = \sum||F_o| - |F_c||/\sum|F_o|$. [b] $wR2 = \{\sum[w(F_o^2 - F_c^2)^2]/\sum[w(F_o^2)^2]\}^{1/2}$ for $I > 2\sigma(I)$. $w = 1/[\sigma^2(F_o^2) + (aP)^2 + bP]$, where P is $[2F_c^2 + \max(F_o^2, 0)]/3$.

refinement of the structure. The asymmetric unit contains two crystallographically inequivalent Ag atoms. Two ligands are situated about crystallographic inversion centers; therefore, only half of each ligand is present in the asymmetric unit. Two independent $(P,Sb)F_6^-$ anion positions were located; however, the PF_6^- and SbF_6^- anions were found to be mixed together on both sites, in the refined proportions P1/Sb1 = 0.314(1)/0.686(1) and P2/Sb2 = 0.467(1)/0.543(1). Refinement of either site as fully P or fully Sb resulted in unreasonably small (P) or large (Sb) displacement parameters as well as higher *R*-values. The fluorine atoms in both anion sites are reasonably ordered, and therefore, the P(Sb)−F bond lengths represent a weighted average of the P−F and Sb−F contributions. The slightly inflated displacement parameters for these fluorine atoms may reflect the presence of two closely separated F_6 octahedra, or simply the rotational disorder commonly encountered in spherical anions of this type. A region of disordered solvent is also present in the crystal, which was modeled as $^1/_4Et_2O$ and $^1/_4CH_3CN$, both disordered about an inversion center. Eventually, all non-H and nonsolvent atoms were refined with anisotropic displacement parameters; the solvent molecules were refined isotropically. A total of 7 geometric restraints were used in modeling the solvent disorder (SHELX SAME and DFIX). Hydrogen atoms were idealized and included as riding atoms.

Systematic absences in the intensity data of **7** uniquely determined the space group $P2_1/c$. All atoms reside on positions of general crystallographic symmetry. The asymmetric unit contains one Ag atom, one ligand, one SbF_6^- counterion, a fully ordered acetone molecule of crystallization, and half of another acetone disordered about an inversion center. Non-hydrogen atoms were refined with anisotropic displacement parameters; hydrogen atoms were idealized and included as riding atoms. At convergence, two relatively large electron density peaks (ca. 4.0 and 3.6 e $Å^{-3}$) located ca. 1 Å from the Sb atom are present. The origin of these peaks is unknown.

The metric parameters of noncovalent interactions ($\pi-\pi$ stacking, C−H···π interactions, and weak hydrogen bonding) were calculated by PLATON.[37] Crystal and refinement data are provided in Table 1 and also in Supporting Information.

Acknowledgment. The authors thank the National Science Foundation (CHE-0110493) for support. We thank Drs. Sherine O. Obare and Latha A. Gearheart for assistance in physical measurements.

Supporting Information Available: X-ray crystallographic files in CIF format, selected bond lengths and angles, and crystal and refinement data for **1**−**7**. This material is available free of charge via the Internet at http://pubs.acs.org.

IC035207I